NOVA SCHOOL OF SCIENCE & TECHNOLOGY

DEPARTAMENT OF MATERIALS SCIENCE

Denis Comlev

BSc in Materials Engineering

MICROSTRUCTURE AND MECHANICAL PROPERTIES OF CERAMICS REINFORCED WITH RECYCLED WASTE

MASTER IN MATERIALS ENGINEERING

NOVA University Lisbon

October, 2023

NOVA SCHOOL OF SCIENCE & TECHNOLOGY

DEPARTAMENT OF MATERIALS SCIENCE

MICROSTRUCTURE AND MECHANICAL PROPERTIES OF CERAMICS REINFORCED WITH RECYCLED WASTE

DENIS COMLEV

Master in Materials Engineering

Adviser: João Pedro Oliveira
Assistant Professor with Habilitation, NOVA University Lisbon
João Pedro Veiga
Associated Professor, NOVA University Lisbon

Examination Committee:

Chair: Doutora Maria Margarida Rolim Augusto Lima,
Professora Auxiliar do Departamento de Ciência dos Materiais da NOVA School of Science and Technology | FCT NOVA

Rapporteurs: Doutora Andreia Filipa Cardoso Ruivo,
Investigadora do VICARTE da NOVA School of Science and Technology | FCT NOVA

Adviser: Doutor João Pedro de Sousa Oliveira,
Professor Auxiliar do Departamento de Ciência dos Materiais da NOVA School of Science and Technology | FCT NOVA

MASTER IN MATERIALS ENGINEERING

NOVA University Lisbon
October, 2023

Dedicated to anyone reading this.

ACKNOWLEDGMENTS

I would like to extend my sincere and utmost gratitude to my supervisors, João Pedro Oliveira, and João Pedro Veiga, for their availability, support, and ambition that was heartfelt by me. Their belief in the project was crucial to its success.

I would also like to thank the University and every professor who had lectured me for their flexibility and support throughout all the strife and hardships, and all the incredible opportunities on and off campus, as well as a fulfilling curriculum every semester.

Furthermore, I would like to thank Professors Margarida Rolim Lima, and Ana Pimentel, for providing help with laboratory procedures, and for helping with the DSC and its usage, respectively.

I wholeheartedly thank Rui Gonçalves for his patience, supervision, and experience with sample manufacture, testing, and details I might have missed throughout this project. I would also like to thank Jiajia Shen for lending a helping hand in optical microscopy and scanning electron microscopy.

Last but most certainly not least, I must thank my friends who would drop everything in their schedules to lend a listening ear and to help. Finally, thank you so much to my girlfriend Luxmi Sharma, for all the unconditional love and support, since I started the curriculum, I would not be the same without you.

"You have within you right now, everything you need to deal with whatever the world can throw at you." - Brian Tracy

ABSTRACT

The recycling of ceramic materials is a challenging task, partly due to the high-energy costs associated with the recycling process itself, as well as future manufacturing stages like fusion and curing. To mitigate the energy expenses of ceramic recycling, it is possible to incorporate ceramic waste into gypsum composites, with the purpose of enhancing their properties while simultaneously benefiting the environment.

By reinforcing gypsum with particles derived from waste, it is possible to shape the reinforced gypsum with the same geometry as pure gypsum, allowing it to maintain its versatility and improve its physical characteristics.

The use of silicon carbide (SiC) particles, a ceramic with high hardness, as reinforcement for gypsum composites, not only represents an effective strategy for repurposing this waste, but also introduces a new material with enhanced mechanical characteristics.

The manufacturing process of this composite reduces the amount of gypsum required and elevates the performance of gypsum to new levels.

With the aim of optimising the use of material resources, this study demonstrates that it is possible to integrate ceramic waste efficiently, promoting more sustainable materials. The success in enhancing gypsum opens the possibility of using ceramic waste in other composites across various contexts.

Keywords: Gypsum, Composites, Sustainable Composites, Material Characterisation.

RESUMO

A reciclagem de materiais cerâmicos é uma tarefa difícil, em parte devido aos elevados custos energéticos associados ao processo de reciclagem em si, assim como futuras etapas de fabricação, como a fusão e a cura. Para reduzir os custos energéticos da reciclagem de cerâmica, é possível implementar resíduos cerâmicos em compósitos de gesso, com o propósito de melhorar as suas propriedades e, ao mesmo tempo, beneficiar o ambiente.

Ao reforçar o gesso com partículas provenientes de resíduos, é possível moldar o gesso reforçado com a mesma geometria que o gesso puro, permitindo manter a sua versatilidade, e melhorando as suas caraterísticas físicas.

O uso de partículas de carbeto de silício (SiC), um cerâmico de elevada dureza, como reforço incorporado em compósitos de gesso, não só representa uma estratégia eficaz de reaproveitamento deste resíduo, mas também introduz um novo material com carateristicas mecânicas aprimoradas.

O processo de manufatura deste compósito reduz a quantidade de gesso necessário, e leva o desempenho do gesso a novos patamares.

Com o objetivo de otimizar o uso de recursos materiais, este estudo demonstra que é possível integrar resíduos cerâmicos de forma eficiente, promovendo materiais mais sustentáveis. O sucesso na melhoria do gesso abre a possibilidade do uso de resíduos cerâmicos em outros compósitos em vários contextos.

Palavras chave: Gesso, Compósitos, Compósitos Sustentáveis, Caraterização de Materiais.

CONTENTS

List of Figures

GLOSSARY

ASTM	Previously "American Society for Testing and Materials", is an organisation that develops and publishes standardisation norms.
DSC/TGA	The combination of DSC and TGA techniques used to characterise thermal performance of a material.
Pa	Pascal, a unit of Force per Area, or Pressure.
SiC	Silicon Carbide, a hard ceramic often used in abrasives, containing Silicon and Carbon atoms.

ACRONYMS

ASTM	Previously "American Society for Testing and Materials"
CMC	Ceramic Matrix Composite
DSC	Differential Scanning Calorimetry
SEM	Scanning Electron Microscope
TGA	Thermogravimetric Analysis

SYMBOLS

σ	Stress, measure of external force over a cross sectional area of an object.
ϵ	Strain, unitless measure of deformation.
E	Young's modulus or elasticity modulus.
ρ	"Rho" used to express density, measure of mass over volume.

1

INTRODUCTION

1.1 Fundamentals

The availability of material resources is finite, and their processing requires significant energy, particularly ceramic materials due to their high processing and curing temperatures. One of the ways to reduce these energy requirements is to reduce the content of new materials, substituting it with a material that is easier to process, or that does not have to be processed.

Monolithic ceramics are high-strength, brittle materials made of a single type of material [1]. One of the biggest problems of monolithic ceramics is their fragility, which leads to catastrophic failure, limiting their usage in high-tech industries. The goal of Ceramic Matrix Composites (CMCs) is typically to enhance the fracture toughness of monolithic ceramics [2].

CMCs are commonly reinforced by fibres, monolithic crystals, layers, or particles. The increase in toughness (hardening) of CMCs is due to the mechanisms of deflection, slippage, closure of defects, and more. While monolithic ceramics experience catastrophic failure, CMCs fail more gracefully thanks to these mechanisms and exhibit significant increases in toughness.

1.2 Composite materials

The revolutionary concept of combining two types of materials with distinct characteristics when isolated, with the goal to enhance the performance of the resulting material from their combination, yielding properties that are unattainable in the individual materials, forms the foundation of composite materials. With these materials, one can achieve combinations of properties that, at first glance, appear contradictory and would not be observed in isolated

materials, such as high tensile strength and low density simultaneously. The properties of various engineering materials are highlighted in Figure 1.1.

Composite materials are typically comprised of a matrix and reinforcement. The matrix is the continuous medium that surrounds the reinforcement. The reinforcement is a discontinuous material embedded within the matrix. Among the various combinations and classifications of composites, there are Ceramic Matrix Composites (CMCs), including ceramics reinforced with ceramics (such as Al_2O_3 reinforced with SiC used in high-tech industry). Reinforcements can be continuous, extending continuously along the length of the composite, or discontinuous, behaving as a set of discrete elements embedded in the matrix [1]. Continuous reinforcements include continuous fibres, usually grouped together and extending throughout the composite's length, or monofilaments, which are larger and isolated from each other. Discontinuous reinforcements take the form of short fibres, similar to continuous fibres, but they do not extend along the length of the composite and do not exhibit the same behaviour; whiskers, which are elongated single crystals; particles, approximately equiaxed reinforcements generally larger than 1 μm; dispersoids, similar to particles but with sizes smaller than 1 μm; and finally, platelets, which are planar reinforcements [1].

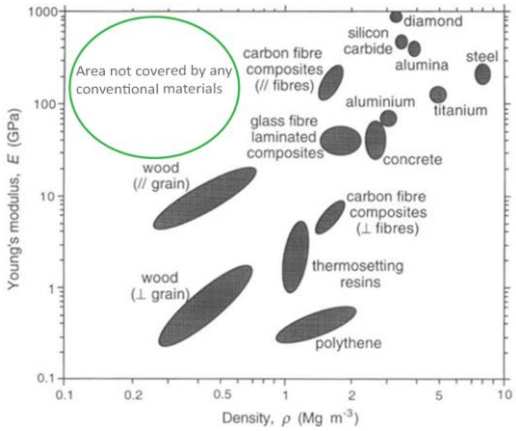

Figure 1.1 Common engineering materials according to their Density and Young's modulus, adapted from [1].

1.3 Ceramic Matrix Composites (CMCs)

Metallic materials are extensively employed and exhibit excellent mechanical characteristics up to their temperature limits, whereupon other materials are necessary due to significantly higher service temperatures. Advanced ceramics are typically low in density, possess high strength, high elasticity modulus, high hardness, strong corrosion resistance, and can maintain their properties at high temperatures. A drawback associated with monolithic ceramics is their fragility, leading to catastrophic failures that limit their use as engineering materials.

Ceramic Matrix Composites (CMCs) are relatively new, advanced materials that are lightweight, exhibit high strength and toughness, maintain these properties at high temperatures, and, unlike monolithic ceramics, demonstrate non-catastrophic failure behaviour when subjected to stress, so they are not brittle. CMCs are designed for extreme conditions where aggressive factors such as high temperatures, stresses, and corrosive environments are combined. These failure mechanisms are attributed to stress transfer from the matrix to the matrix-reinforcement interfaces, preventing catastrophic matrix failure [2], [3].

Ceramic composites play a critical role in extreme temperature scenarios and drive technological advancements in industries like aerospace propulsion, space industry, land transportation, and the chemical and nuclear sectors. CMCs find applications in various advanced engines, gas turbines for power generation, heat exchangers, gas filters, thermal treatments, nuclear fusion reactors, biomaterials, cutting tools, high-precision spherical bearings in corrosive environments, and more [2], [3].

The categorisation of different types of CMCs can be carried out based on the matrix and reinforcement composition, such as oxides, non-oxides, and glasses, resulting in classifications such as: Non-oxide/non-oxide composites when both matrix and reinforcement are non-oxide ceramics; Non-oxide/oxide where the matrix is non-oxide and the reinforcement is oxide, or vice versa; Oxide/oxide when both are oxides; Glass and Glass-Ceramics where the matrix is a glass or glass-ceramic [2].

The behaviour of CMCs is strongly related to the reinforcements used. Reinforcements based on non-oxide fibres like carbon or silicon carbide exhibit superior mechanical properties at high temperatures but are vulnerable to oxidation. Oxide-based fibre reinforcements (such as alumina) are oxidation-resistant and possess good mechanical properties but lose these qualities at elevated temperatures [2].

Contrary to PMCs or MMCs, in which reinforcements are stiffer and undergo failure before the matrix, the brittle matrix fails first in CMCs, hence the necessity of stress deflection at the matrix-fibre interface. This deflection involves deliberately weakening the matrix-fibre bond, often achieved by introducing a thin layer of weak matrix on the fibre surface. This process causes the fibres to function as a weaker link that fails earlier than the matrix [3]. The intentional weakening of these matrix-fibre connections allows CMCs to experience damage during loading, exposing the fibres to the atmosphere. These mechanisms are responsible for the material's toughness, a characteristic uncommon in ceramic materials. Proper processing of CMCs is essential to avoid fibre degradation [3].

Previously, other authors have observed that the addition of a second phase to ZrC improves sintering properties, normalises matrix particle growth, and enhances the strength and toughness of the ceramic. Various preparation technologies include pressureless sintering, hot pressing, and spark plasma sintering [4]. Mechanisms for ceramic hardening include grain pinning with additives like ZrB_2, resulting in a finer grain size and a more homogeneous microstructure. Deflection of defects and additive clusters also contribute to increased ceramic toughness. However, it is crucial to note that excessively small or large additives can be detrimental, affecting the deflection of defects [4], [5], [6].

1.4 Effects of SiC additives on gypsum hydration and crystallisation

SiC micro and nano powders have already shown promise in accelerating gypsum hydration as well as increasing the size and length of its crystals [7]. In the mentioned study, crystal length increases as SiC additive size is decreased, starting at 3 to 5 mm for gypsum crystals grown without additives, 5 to 7 mm when micro additives are added, and 7 to 9 mm when nano additives are added instead. Width also increases from 0,1 mm with no additives, to 0,2 mm with micro additives, and 0,6-0,8 mm with nano additives.

The microstructure of a material, such as crystal shape and size, is heavily linked to its macroscopic properties, such as flexural strength.

1.5 Chapter conclusions

Considering the issues related to ceramic material recycling, and the necessity to move into sustainable development, this study explores the potential of improvements on mechanical properties and the microstructure changes in ceramics reinforced with recycled waste.

Not only does the integration of recycled waste hold energy saving promises, but it also presents an opportunity to improve the performance of currently available ceramics.

While particle reinforcement has been mostly limited in its applications, the low energy entrance fee is a significant advantage in making these composite materials more economically viable.

The results of this study draw parallels to CMCs with other types of matrices that utilize waste particles as reinforcement, similar to the expensive ultra-high-temperature ceramics employed in the high-technology sectors mentioned above [4].

2

MATERIALS AND METHODS

2.1 Specimen fabrication procedure

The matrix of the composite is made of commercial gypsum-based adhesive for plasterboards, with calcium sulphate hemihydrate as its main component in powder form. With the addition of water, it is possible to fabricate solid samples with calcium sulphate dihydrate according to eq. 1 [8].

$$CaSO_4 \cdot 2H_2O \leftrightarrows CaSO_4 \cdot 1/2H_2O + 3/2H_2O \quad (1)$$

The reinforcements consist of hard ceramic particles of recycled SiC. The recycled SiC consists of both angular and spherical particles with an average diameter of 9 μm. A barrel of recycled SiC particles of similar size was used as a source. Microscopy allows for confirmation of average particle size, and pycnometry and X-ray diffraction are techniques that can be used to confirm the purity of the particles. Silicon carbide is often used as abrasive materials for multiple applications, such as sandpapers, braking systems, and cutting tools.

For testing following ASTM D790 [9] and ASTM C1341 [10] standards, specimens of dimension 180 x 30 x 10 mm were fabricated.

A mixture of 57,2 g of gypsum with 35,75 g of water (62,5% water-to-plaster ratio) is necessary to create a single specimen of pure gypsum. This ratio was chosen since gypsum samples created this way are both easy to mix, and quickly dry. Higher water content makes a mixture easier to mix, but take longer to dry, and lower water content makes a mixture harder to mix, but it will dry faster.

To fabricate a specimen, water is added to the mixture of gypsum with reinforcement and then thoroughly mixed for roughly a minute using common housework or gardening tools

to homogenise, followed by a three-minute waiting period for gypsum hydration to take place, making the mixture more consistent.

Wooden boards were used to create appropriately sized spaces where the mixture was inserted into. The floor of these wooden boards included a thin acrylic layer to ensure a smooth finish on one of the surfaces of each specimen for the purposes of a three-point flexural test.

Samples were created for standardisation of tests, verifying the effects of cure time (between 24 hours and 30 days) and reinforcement concentration (either 1,5 or 4,5 %(V/V)) on mass and strength.

Following standardisation, samples were created for different reinforcement concentrations (3 to 19,5 %(V/V)) to determine the optimal reinforcement concentration.

2.2 Three-point flexural test

To determine the maximum strength of each specimen, three-point flexural tests were performed. The support span for the specimens were 160 mm [1], [9], [10].

A three-point flexural test machine available at the laboratory was used to perform these tests. The probe advances at a constant speed of 2 mm/min and values of strength are registered at 0,00625 mm intervals [11].

2.3 Optical microscope

Optical microscope allows for study of reinforcement adhesion to the matrix, as well as microstructure of the composite. For this purpose, a Leica DMI 5000 M inverted optical microscope was used for optical microscopy.

2.4 Scanning electron microscope

A model TM3030Plus scanning electron microscope (SEM) was used to characterise the microstructure of the composite at a higher resolution, which may be hard to detect through optical microscopy.

2.5 Thermogravimetric analysis/ Differential scanning calorimetry

Thermogravimetric analysis (TGA) and differential scanning calorimetry (DSC) were used for thermal analysis through weight changes as temperature increases.

TGA/ DSC was performed in the temperature interval of ambient to 1100 °C, ramping at a constant rate of 5 °C per minute. In addition, an inert atmosphere is required to avoid SiC oxidation [8], [12], [13].

3

RESULTS AND DISCUSSION

3.1 Gypsum performance over curing time

The performance of gypsum samples significantly varies over time. As such, the need for standardisation of time to test samples after manufacture arises. Mass is measured at manufacture time and after 24-hour intervals. Maximum strength is obtained from three-point flexural tests.

Manufacture and testing of samples for the purpose of standardisation started on May 8th, 2023, and ended on June 5th, 2023. Temperature conditions for the manufacture periods can be found in Figure 3.4 and Figure 3.5.

Figure 3.1 shows the evolution of mass over time, varying reinforcement concentration. During the first 48 hours, mass reduces significantly due to evaporation of excess water, which later appears to stabilise and only suffers slight deviations after four days. Reinforcement concentration does not appear to affect the curing process significantly.

Maximum strength over time (Figure 3.2) shows that strength does not further increase significantly after three days, though still increasing at a slower pace. Initial testing was done in sunny, low humidity conditions. Further samples were also tested on colder, more humid days. The considerable variability and significantly lower results observed for day 7 measurements in Figure 3.2 may be attributed to issues such as poor sample mixture, sample slipping during testing, or other problems within those batches. To address this, new samples were generated to rectify the discrepancy in the trend. However, the results remained highly variable and did not align with the expected trend of increasing strength over time. Notably, because these samples were created and cured in open-air conditions, there was substantial variation

in temperature and humidity, making it challenging to replicate consistent conditions for testing new samples under the same reinforcement and time parameters as the previous ones.

Samples manufactured and tested in colder and more humid weather perform significantly worse than the ones done in warm and dry weather, requiring more time to dry for the mechanical testing data to be valid. These results indicate that the measurements heavily depend on temperature, humidity, and sun irradiance.

Having the mass and strength measurements over time, further three-point flexural tests were performed four days after manufacture for the purposes of a standardised period. However, this period depends on weather conditions.

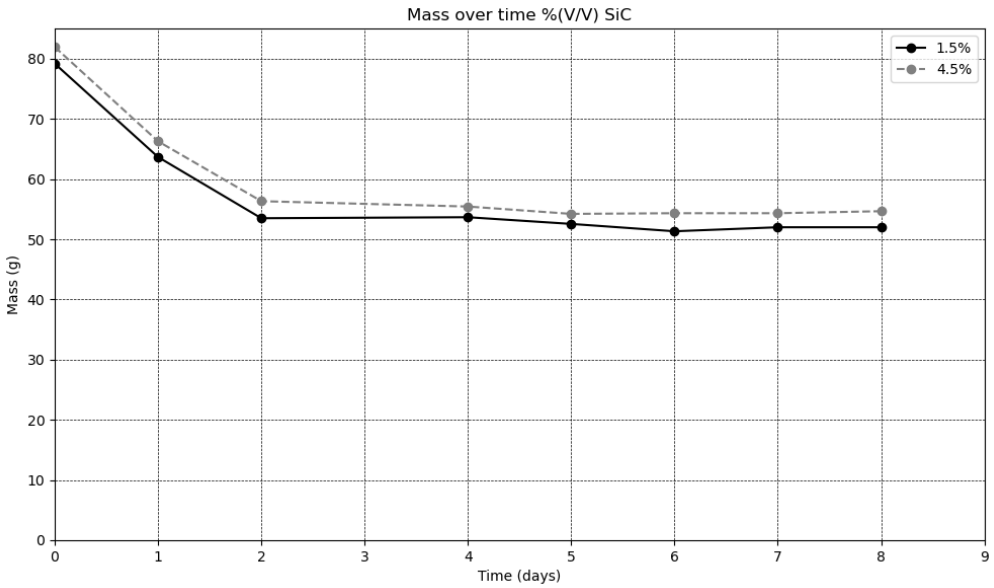

Figure 3.1 Mass over time for different reinforcement concentration.

Individual results for performance over curing time are presented in Figure 4.3 through Figure 4.6.

Other studies have shown that the addition of a micro SiC solution increases hydration temperature, which translates to better, more efficient hydration of gypsum, which can lead to structurally stronger samples [7].

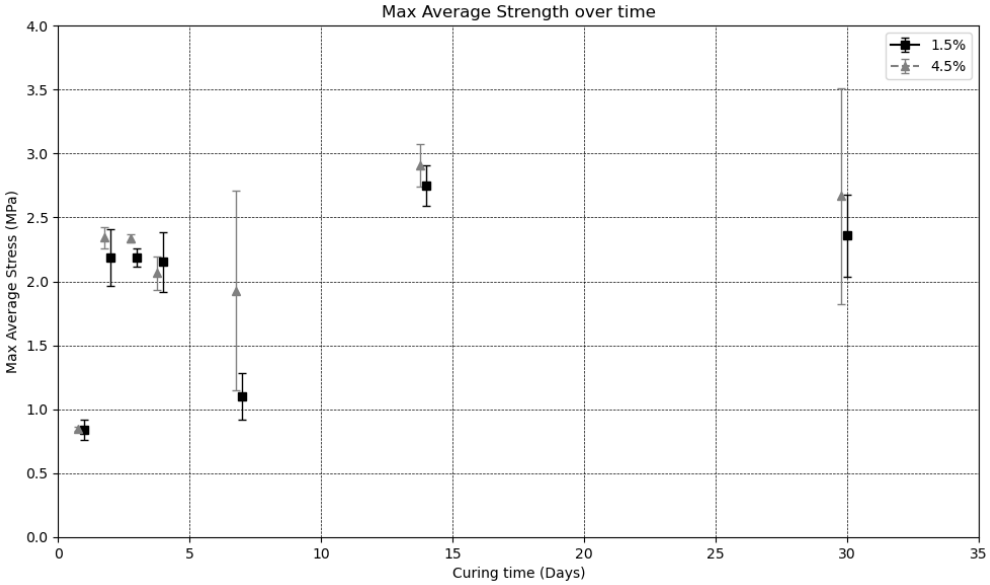

Figure 3.2 Maximum average strength over time for two different SiC %(V/V) concentration.

3.2 Gypsum performance over reinforcement concentration

As reinforcement concentration increases, mixtures become harder to mix, being noticeably more viscous at higher (notably over 10,5 %(V/V)) reinforcement concentrations, which limits mixing equipment that can safely be used.

Manufacture and testing of samples for the study of performance depending on reinforcement concentration was done from July 24th to July 28th, 2023, for some concentrations. Other select concentrations were manufactured from September 7th to September 11th, 2023, and another batch from September 20th to September 26th, 2023, due to severe under-performance from the first batch at some concentrations. A final batch was manufactured from October 2nd to October 9th, 2023, to obtain further results on high concentration samples. Three-point flexural strength results are plotted in Figure 3.3.

The issues with one of the batches that severely under-performed likely come the fact that their curing process included cold and rainy days, hence a longer curing time was decided on for further batches.

Since some samples were manufactured considerably after the first ones, the 5 Kg gypsum bag from where the matrix is sourced had remained open, which exposes it to ambient humidity. Exposure to the air humidity converts some of the plaster into its hydrated counterpart, which affects the quality, and consequently the performance of the samples [8].

Samples become darker as reinforcement concentrations increases, going from white and smooth to the touch samples of pure gypsum (0 %(V/V)) to progressively darker and rougher to the touch specimen (more noticeable at 19,5 %(V/V)), also becoming progressively harder to sand into a smooth finish.

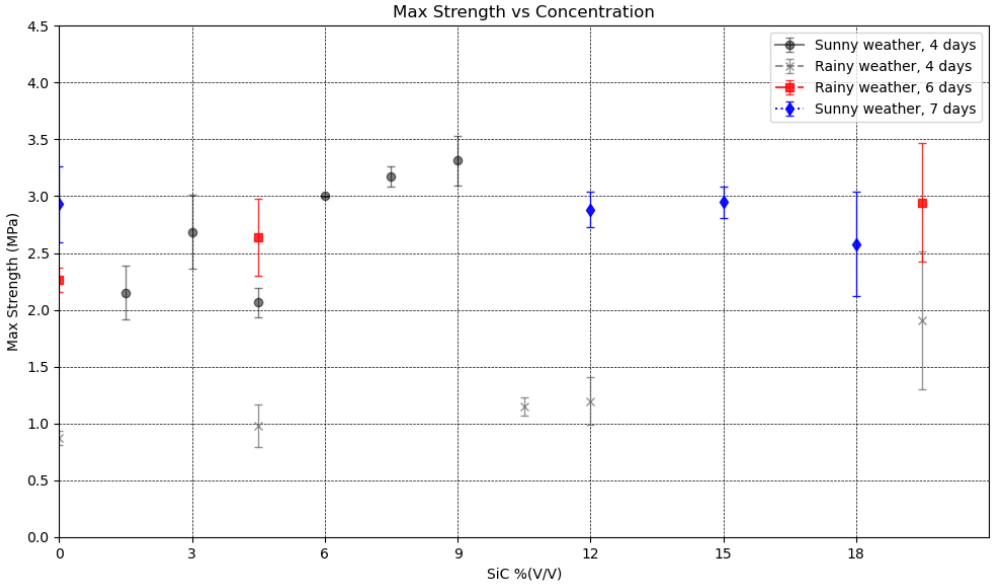

Figure 3.3 Maximum Strength in MPa for different material concentrations, manufactured in batches.

The final batch contained samples of pure gypsum, 12, 15, and 18 %(V/V) SiC. This batch suggests that there is a reinforcement saturation point, where mechanical performance starts to decrease instead of increasing further, located between 12 and 18 %(V/V) SiC, since there is an increase from 12 to 15 %(V/V), but a decrease in the average Maximum Strength from 15 to 18 %(V/V) under the same conditions.

Results for every individual batch can be observed in Figure 4.7 through Figure 4.11.

3.3 Three-point flexural test conclusions

Gypsum under stress often presents steps in the graph where stress remains constant while strain increases. The largest step usually appears at the 1.5 MPa when the samples have been properly dried. This large step does not appear to depend on reinforcement concentration, being present in even pure gypsum samples. This step is associated to failures in the matrix [14].

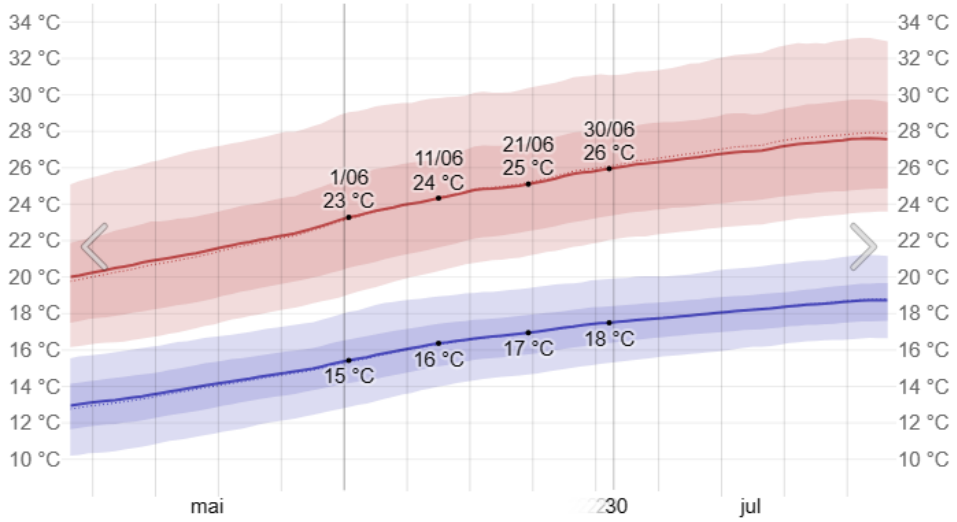

Figure 3.4 Maximum and minimum temperatures in Caparica courtesy of Weatherspark.com.

The presence of a saturation point where mechanical performance starts to decrease suggests reinforcement-to-matrix adhesion issues, as well as bridging of reinforcement particles, creating a shorter path for stresses to travel, as opposed to adding obstacles that deflect said stresses.

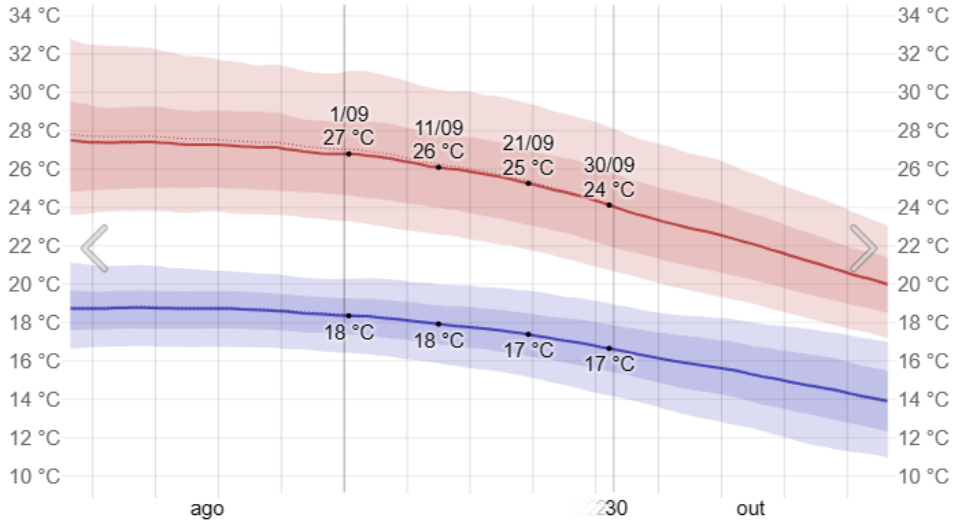

Figure 3.5 Maximum and minimum temperatures in Caparica courtesy of Weatherspark.com.

3.4 Optical microscope images

Samples were taken to the microscope and pictures were taken at different magnification levels. Some of the best and worst performing samples are highlighted in this section.

At smaller reinforcement concentration, such as in Figure 3.6, SiC particles appear to become fully enveloped by the plaster matrix more often, as opposed to higher SiC

concentrations as seen in Figure 3.7, where SiC particles can be seen sticking out, possibly hindering its performance.

Samples in Figure 3.8 and Figure 3.9 were some of the best-performing ones in their group of three, both with 4,5 %(V/V) SiC. These microscope images exhibit favourable distribution of the reinforcement, suggesting that it's been better mixed than others.

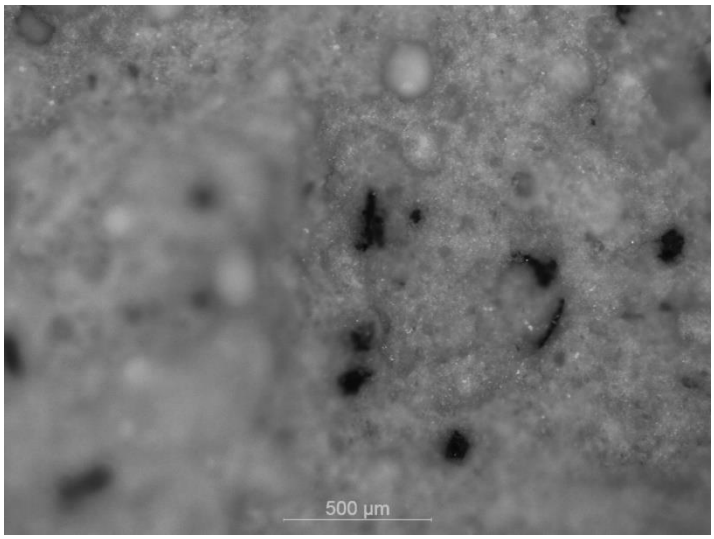

Figure 3.6 Optical microscope image of 1.5 %(V/V) SiC sample where black SiC particles appear to be fully enveloped by the plaster matrix.

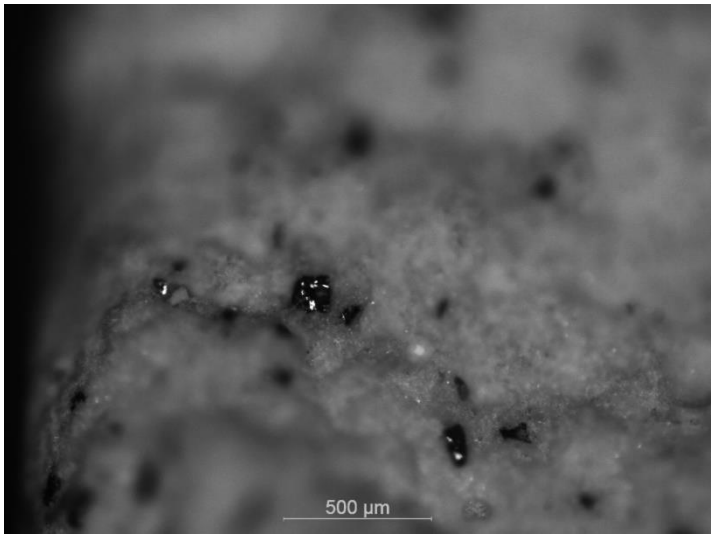

Figure 3.7 Image of 4,5 %(V/V) SiC sample with SiC particles only partially enveloped by the matrix.

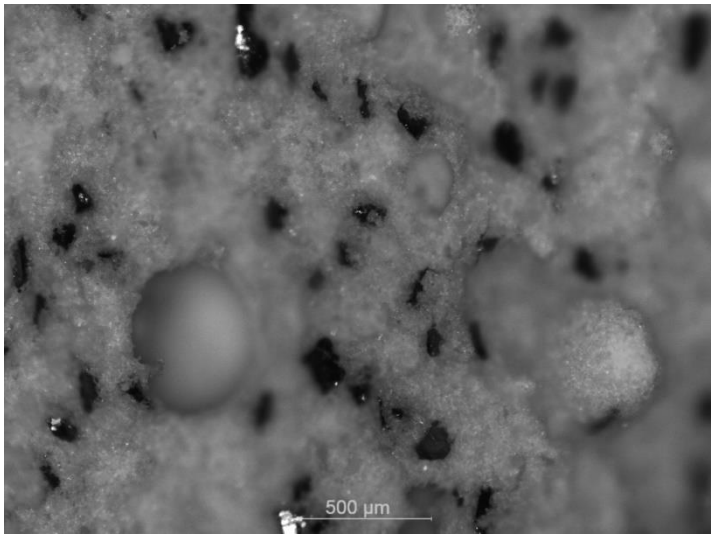

Figure 3.8 Image of well-performing 4,5 %(V/V) SiC where good distribution of SiC particles is present.

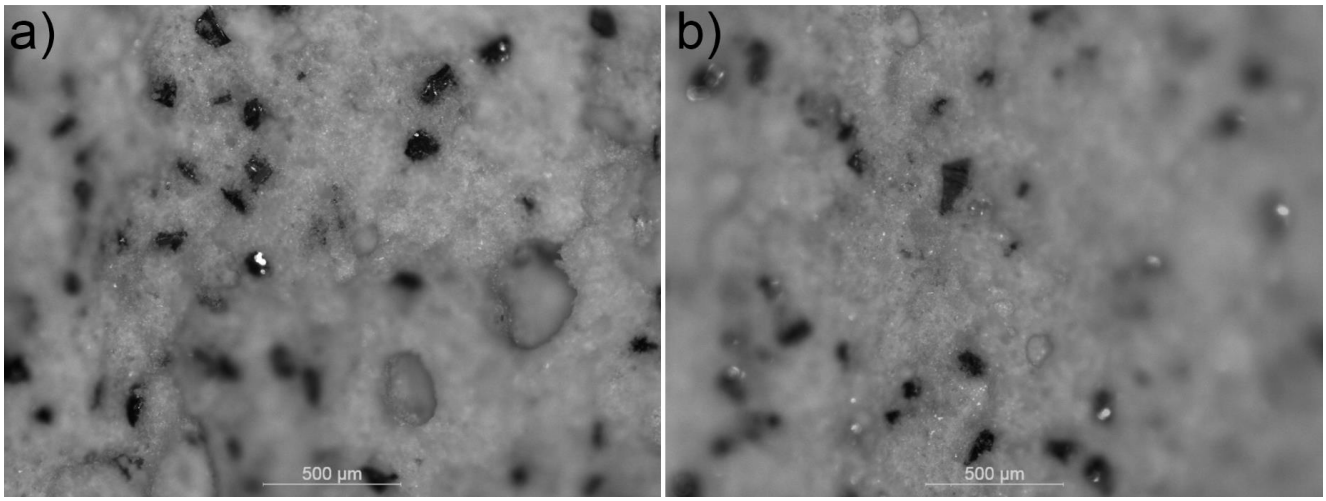

Figure 3.9 Images of best-performing 4,5 %(V/V) SiC samples with evenly distributed well-enveloped reinforcement.

Large voids and highly spherical shapes can be seen in Figure 3.10. These defects negatively affect mechanical performance when near to the testing area. The presence of voids and spheres can be attributed to the incorporation of air pockets during manufacturing. Unhydrated gypsum is another reason for the presence of these spheres [7]. The microstructure of pure gypsum under the optical microscope is evidenced in Figure 3.11.

Pictures of the surface with a good finish of pure gypsum and samples of progressively more reinforcement content concentration is shown in Figure 3.12. Silicon carbide particles remain fully enveloped even at higher concentrations, and the surface remains smooth to the touch.

Sometimes the well finished surface gets stuck to the acrylic layer, exposing a grainy and rough surface instead of the smooth surface wanted. Microscope pictures were taken

inside the circled areas shown in Figure 3.13 for the purpose of showing the exposed surface in Figure 3.14, and covered surfaces mentioned above.

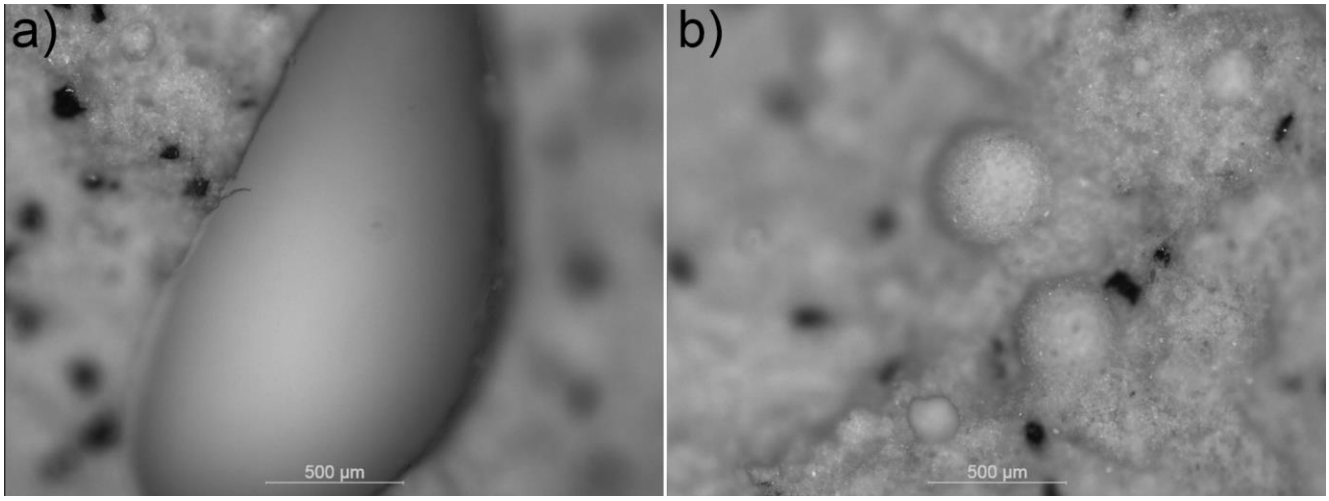

Figure 3.10 Images of a large void on the outer part of a sample (a) and highly spherical shapes attributed to either gypsum that was not hydrated, or the presence of air pockets within the mixture (b).

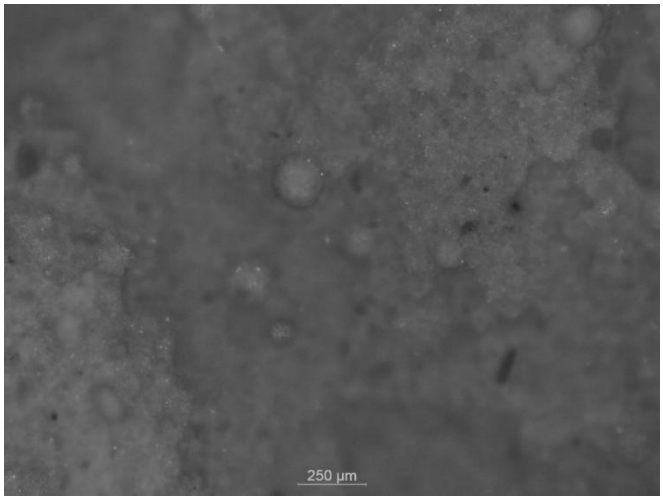

Figure 3.11 Crystalline microstructure of pure gypsum.

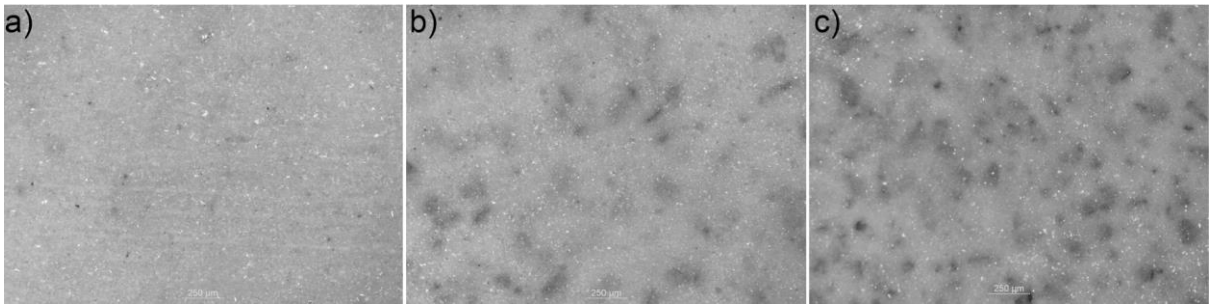

Figure 3.12 Well finished surface of pure gypsum (a) and progressively more SiC content, at 4,5 %(V/V) (b) and 19,5 %(V/V) (c).

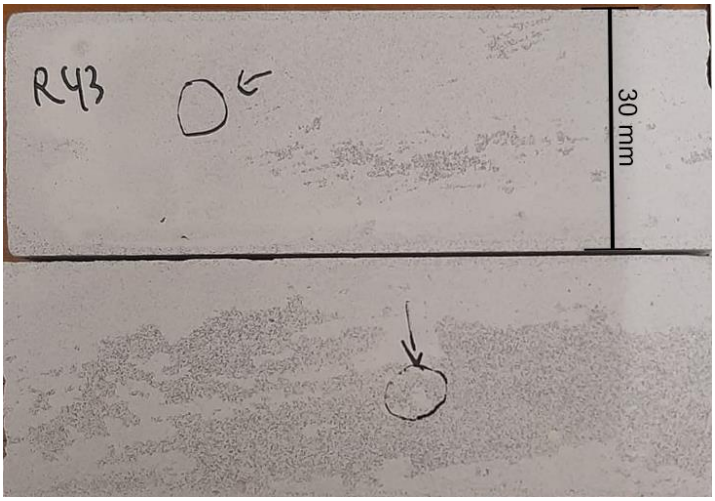

Figure 3.13 Areas that were examined under microscope for the well-finished surface (above) and rough surface (below), when the sample stays stuck to the acrylic layer floor during manufacture.

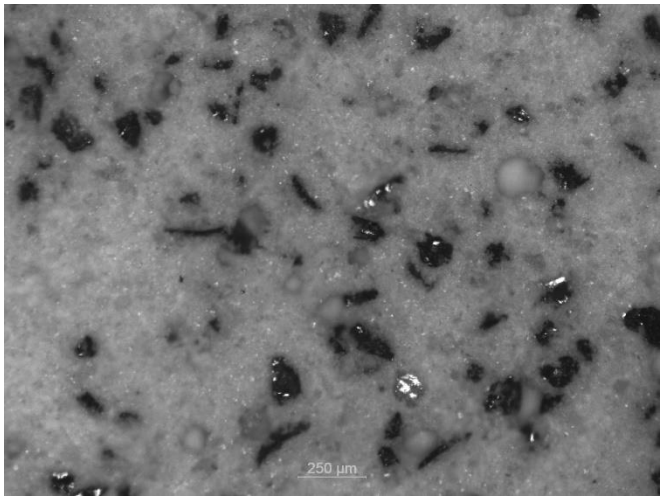

Figure 3.14 Exposed surface of 4,5 %(V/V) sample.

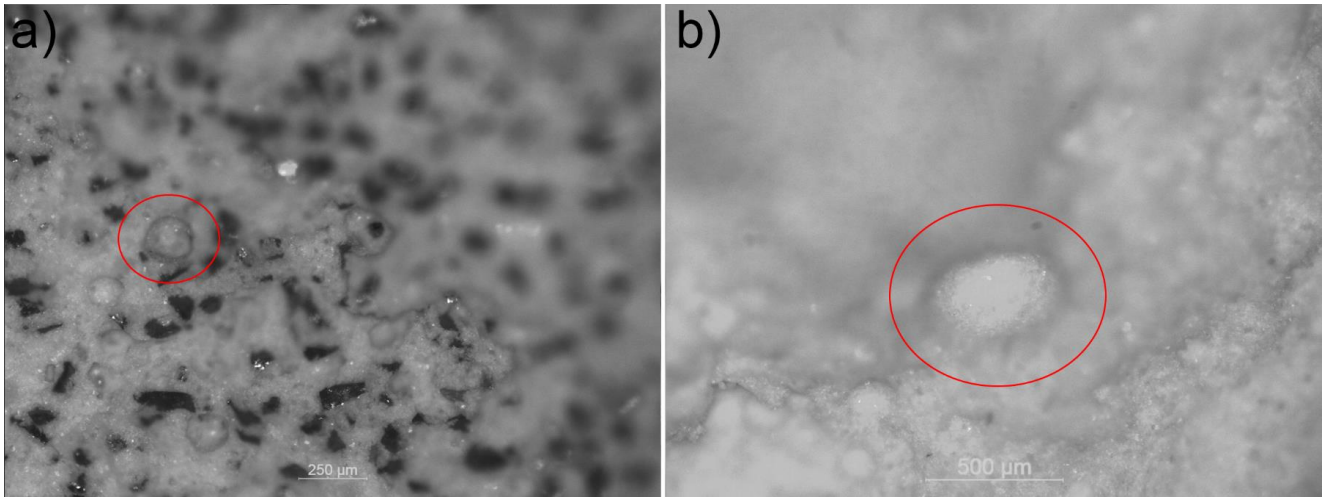

Figure 3.15 Evidence of smaller spherical shapes due to poor hydration when SiC content is high (19,5% (V/V) in a) when compared to lower or no contents of SiC (pure gypsum in b).

Spherical shapes due to poor hydration are both smaller, and harder to find in the fracture area in samples with higher SiC content, such as 19,5 %(V/V) SiC in Figure 3.15.a, compared to samples with less, or no SiC, such as in pure gypsum in Figure 3.15.b. Increase in SiC content correlates to a discernible reduction in both quantity, and size of defects, suggesting better gypsum hydration as SiC content increases.

Silicon carbide particles can be seen partially exposed, where they are easier to spot, or heavily enveloped by the gypsum matrix, both cases observable under the microscope in Figure 3.16. Reinforcement particles can be clearly visible in the fracture area, suggesting that these are tension concentration points, where the material is weakest and fails first.

A strategy to improve performance of Fiber Reinforced Composites is the weakening of the Fibre-Matrix interface to avoid failure of the composite, avoiding brittle failure as well [3]. Since SiC is stronger and harder than gypsum, stress failure of the particles is unlikely. However, the interface between the particles and the matrix seems to be a common weak spot, as seen in Figure 3.17.

Tensile strength improvements may be related to the interactions between the reinforcement/ matrix and the failure mechanism, in addition to matrix hydration improvements. One problem that can occur at higher reinforcement concentrations is the bridging of stress between particles, creating a clear path for stress to progress through the material, leading to diminishing returns in some cases, and even worsening tensile strength in the worst cases. Figure 3.17.b shows that SiC particles that are in proximity can create short paths for stress to travel through.

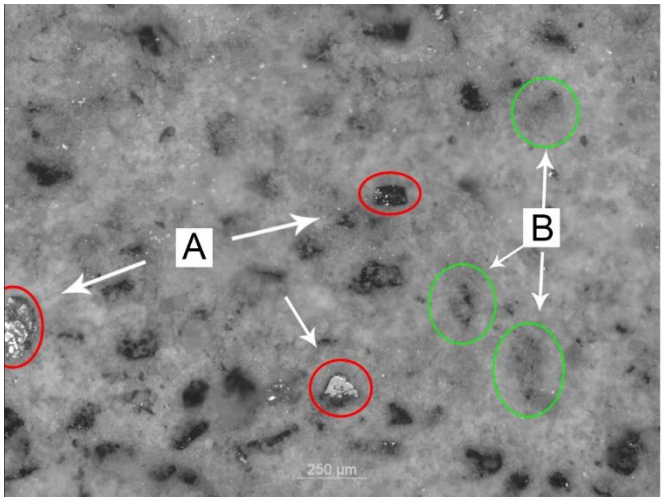

Figure 3.16 Sample with 19,5 %(V/V) SiC where some SiC is heavily enveloped (B) and some is cleanly exposed (A).

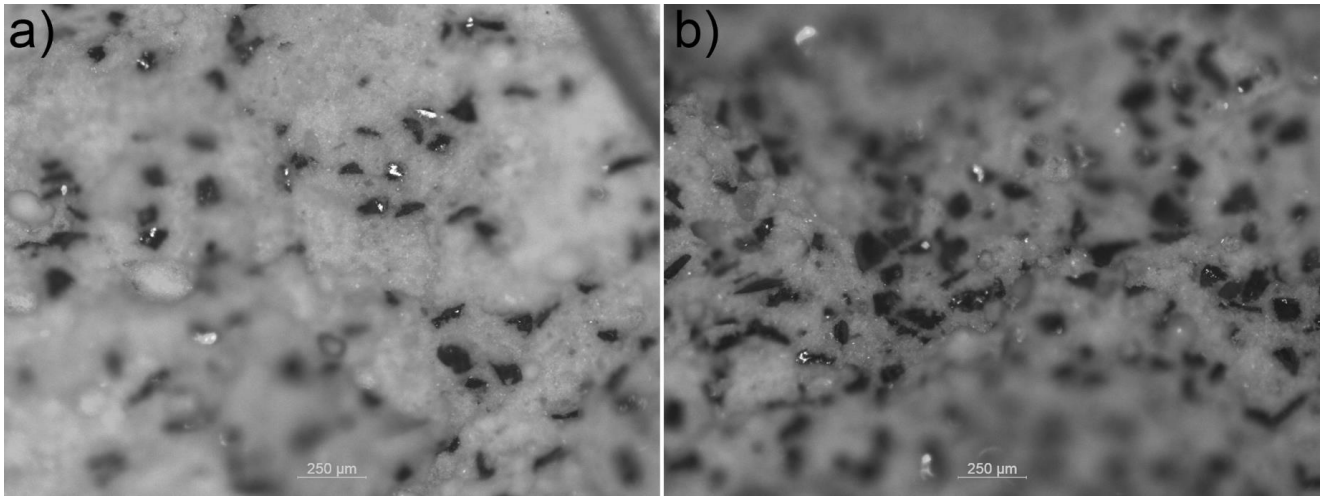

Figure 3.17 Microscope pictures of fracture site for 4,5 %(V/V) SiC (a) and 19,5 %(V/V) SiC (b) where reinforcement/ matrix interface appears to be a weak spot.

The usage of a regular vibrating table, such as ones used for concrete casting, could further help mixing which would reduce the variability of results, as well as improving the overall performance of samples [15], [16].

3.5 SEM analysis

Scanning electron microscope (SEM) provides pictures of greater resolution than optical microscopy, allowing for a more detailed study of the microstructure of the composite and matrix adhesion of the reinforcement particles.

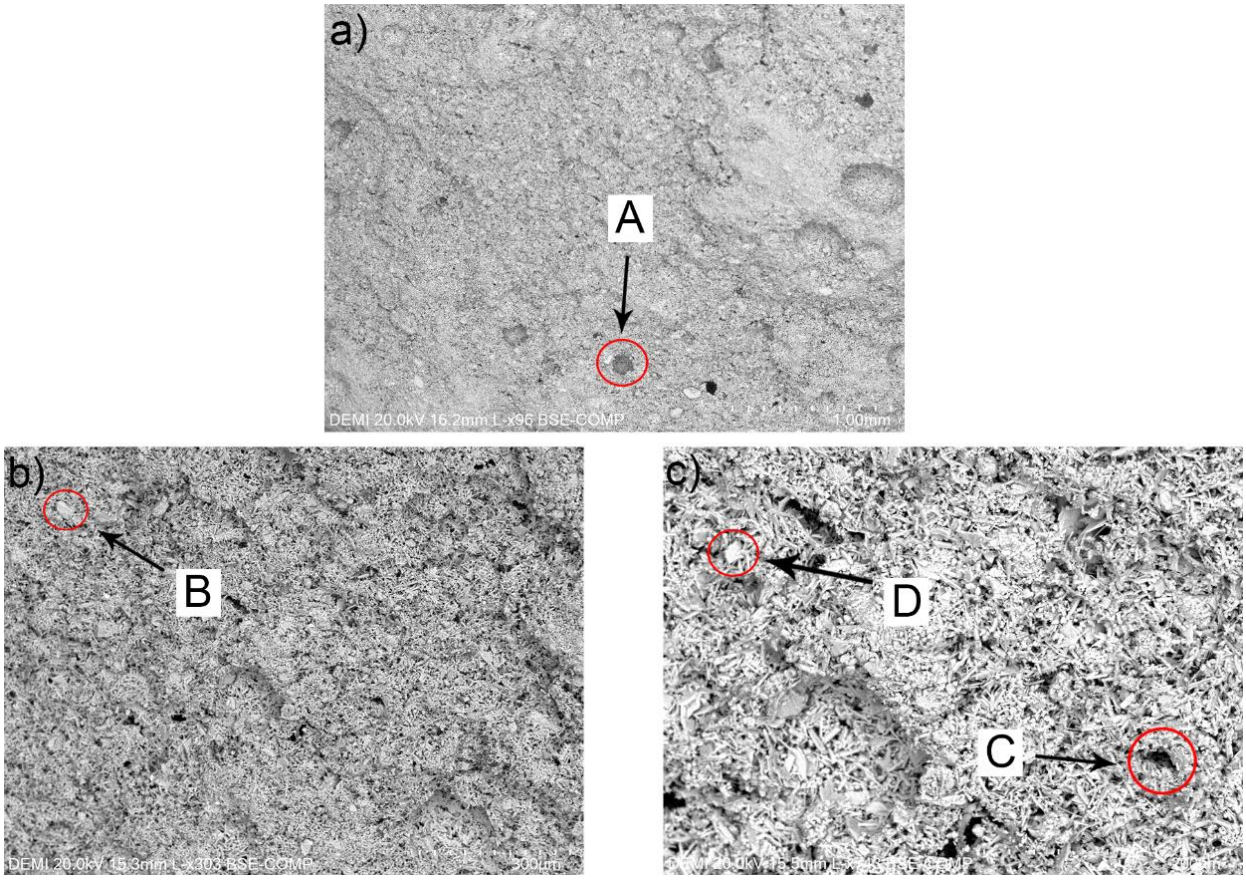

Figure 3.18 SEM images of fracture sites for a pure gypsum sample.

Some types of defects are universally present in failure sites, such as the ones seen in Figure 3.18. These defects are intrinsic to the sample fabrication process. Defects highlighted as A and C are voids in the material due to air pockets that remain through fabrication, and defects B and D are instances of non-hydrated gypsum. As evidenced from their presence on the fracture surface, these defects are weak points of the material and negatively affect its mechanical properties.

Gypsum microstructure is crystalline and made up of elongated, needle shaped crystals.

In the presence of SiC, the fracture site starts to show an increase in reinforcement content. SiC particles can be detected in the microscope images due to their larger size when compared to gypsum's needle shaped crystals, since SiC particles have large edges and surfaces, as seen in Figure 3.19. The fact that the edges of SiC particles remain in the fracture site shows that there may be problems of matrix adherence to the reinforcement, as the weakest part of the material locally was the interface between an SiC particle and the gypsum matrix, letting the stress to progress. Further increase of SiC content is expected to also improve mechanical performance, however, the possibility of reinforcement particles bridging together and negatively affecting the performance of the material is a possibility.

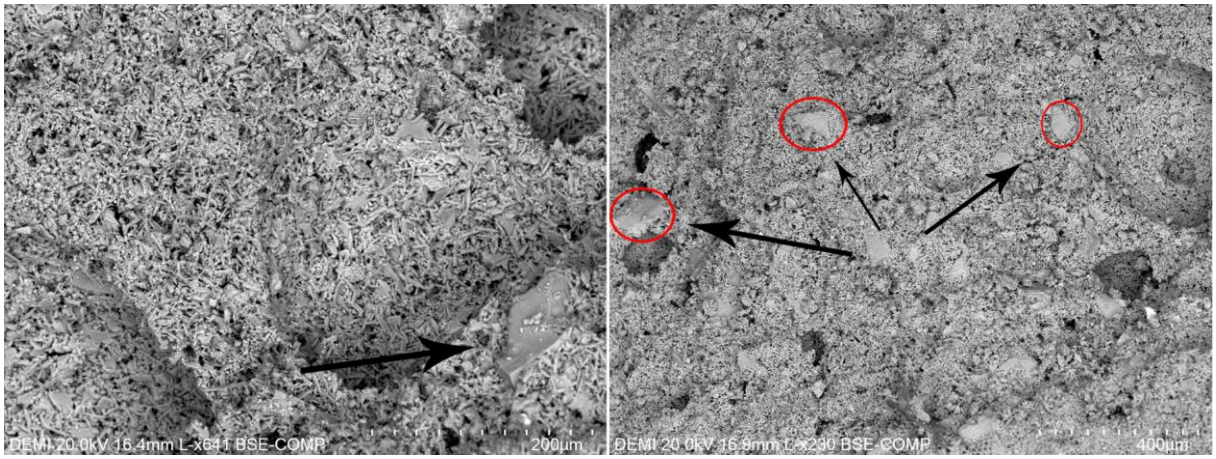

Figure 3.19 Sem images of 9% (V/V) SiC sample's fracture site.

SEM pictures of the failure site of the 19,5 %(V/V) SiC samples were also taken. The presence of voids remains a major factor in the location of the shortest stress path, SiC particles can be seen across the fracture site in Figure 3.20.

Figure 3.20 SEM image of 19,5 %(V/V) SiC sample's fracture site.

SEM images of very high reinforcement concentration samples, such as Figure 3.21, show that high levels of reinforcement also lower distance between reinforcement particles significantly, to a point where said stresses can move through weak matrix-reinforcement interfaces easily.

Stresses will often travel through the shortest and weakest paths, as such, approximately straight paths can be seen between reinforcement particles across optical and scanning electron microscopy images, such as Figure 3.21.b.

Gypsum crystals are expected to increase in size, becoming longer and thicker than pure gypsum crystals [7]. However, these differences are hard to find in the optical microscopy and SEM pictures taken.

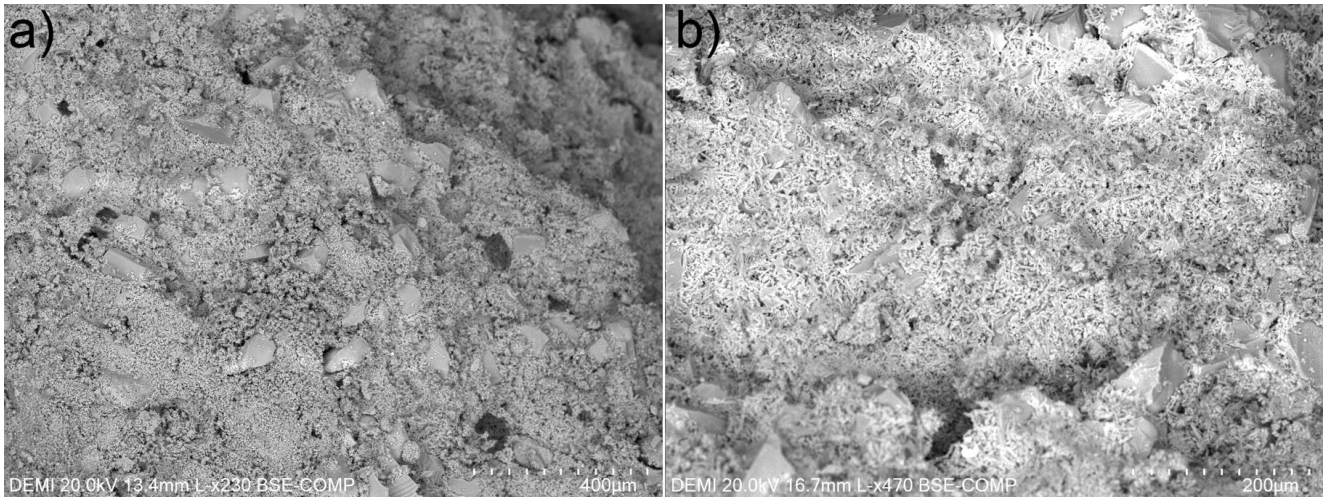

Figure 3.21 SEM images of 19,5 %(V/V) SiC sample's fracture site.

3.6 Thermogravimetric Analysis/ Differential Scanning Calorimetry

TGA/ DSC was performed on a pure gypsum sample, a 9 %(V/V) SiC sample, and a 19,5 %(V/V) SiC sample, seen in Figure 3.22, Figure 3.23 and Figure 3.24 respectively, with a temperature range of ambient to 1100 °C, temperature rate of 5°C/ min at inert atmosphere. SiC has very high thermal stability and does not begin to decompose in the temperature range used for these tes[17].

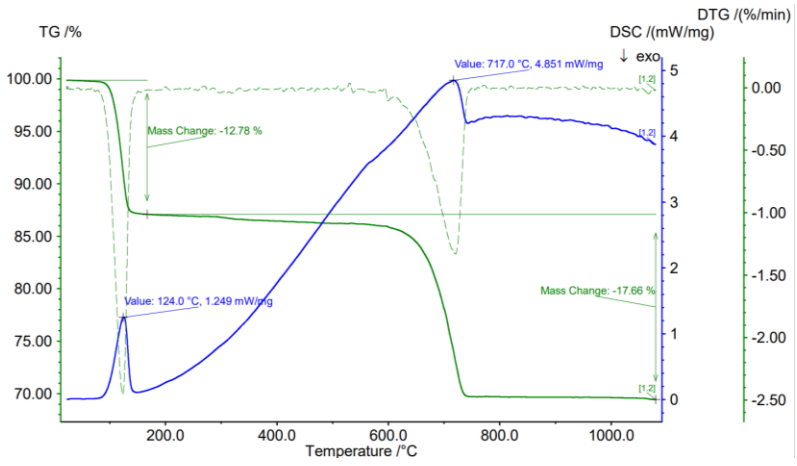

Figure 3.22 TGA/ DSC results for pure gypsum sample.

The first notable reaction is an endothermic reaction occurring up to ~130 °C, associated with the dehydration of the sample, where bound water molecules are released from the gypsum crystalline structure. The first dehydration temperature is approximately equal for all samples, at either 124 or 122 °C.

The mass loss for the pure gypsum sample is higher than the reinforced ones, since silicon carbide particles are stable throughout the test, and are also denser than gypsum, hence a lower portion of the mass is lost for the reinforced sample. Energy consumption associated with this dehydration is consequently higher for the pure gypsum sample, since a larger portion of the sample reacts.

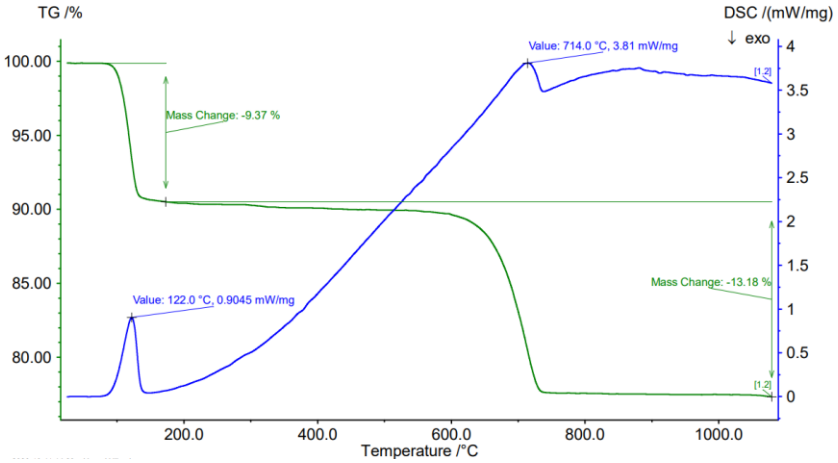

Figure 3.23 TGA/ DSC results for 9 %(V/V) SiC gypsum sample.

One of the reactions where the results overlap is a step starting at ~600 °C. This is a calcination reaction commonly seen in gypsum, evidenced below in eq. 2 [18].

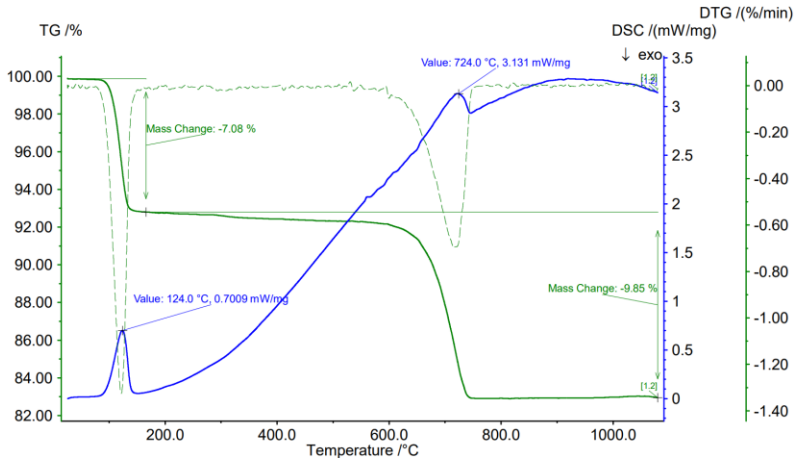

Figure 3.24 TGA/ DSC results for 19,5 %(V/V) SiC gypsum sample.

$$CaSO_4 \cdot \frac{1}{2}\mathrm{H_2}O \rightarrow CaSO_4 + \frac{1}{2}H_2O \quad (2)$$

Results overlap with most of the graph. However, the samples differ in the reaction occurring at ~715 °C. This reaction (evidenced in eq. 3) is associated with the decomposition of $CaCO_3$ [18] and peaks at 717 °C for the pure gypsum sample, 714 °C (-3 °C) for 9 %(V/V) and at 724 °C (+7 °C) for the 19,5 %(V/V) SiC reinforced sample.

$$CaCO_3 \rightarrow CaO + CO_2 \quad (3)$$

This shift to higher temperatures in the presence of high contents of SiC means that more energy is required for the calcination reaction, which can mean better thermal stability. One reason for this shift, in addition to the fact that impurity content is increased, can be the increased gypsum crystal size, which decreases reactivity and requires more energy for the same calcination process. However, positive effects appear to only be present in higher reinforcement concentration, since for a 9 %(V/V) reinforcement sample the reaction occurs at a similar, slightly lower (-3 °C) temperature.

4

Conclusions and Future Perspectives

Usage of a controlled environment for further development is preferred, especially in environments with high variability in temperature, humidity, and sun irradiance.

Manufacture of samples by hand and resorting to sunlight does come at a lower energy cost, however, a controlled environment and appropriate equipment, such as a drying oven, a vibrating table, and a mechanised mixer, can create samples with less variance, and better results in mechanical performance, when said equipment is available.

The use of different types of fibre reinforcements [11], [16], [17], [18] in addition to particles can improve the materials mechanical properties at a macroscopic level, while also leading to more efficient hydration.

Furthermore, machine wear and tear can increase variability over time, and increases in gypsum source humidity can lower its quality, as well as increase variability in mechanical testing [8][.

SiC micro and nano additives may contribute positively to the mechanical performance, since gypsum crystals grown this way are larger and stronger [7].

Improvements in gypsum composites from particle reinforcement by itself may be limited, however, the effects of silicon carbide on the microstructure and hydration of gypsum are promising.

Failure near silicon carbide reinforcement particles points to it being a weak point in the composite, where stress can progress easily. Allowing stresses to be intersected by the SiC-Gypsum interface delays brittle failure, allowing the composite to fail more gracefully than the isolated matrix would.

SiC particles hence serve as obstacles to stress, increasing the energy necessary for them to travel from one end of the material into the other, while also absorbing energy when interacting with the weak reinforcement-matrix interface (Figure 4.1).

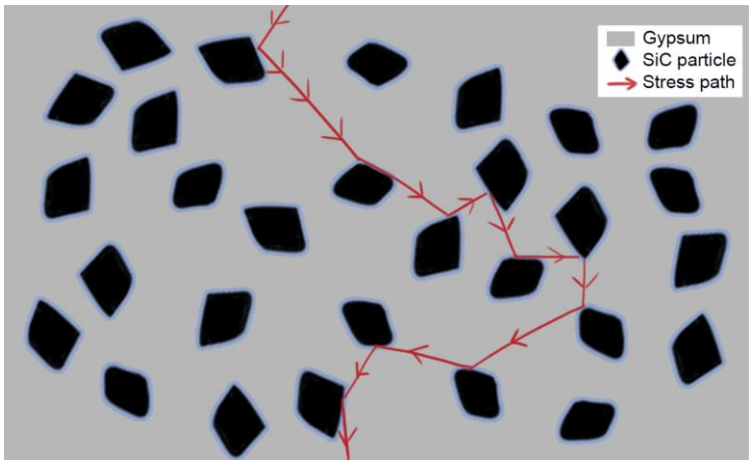

Figure 4.1 Effect of SiC particles and their interfaces on stress travelling through a gypsum sample.

An excess of reinforcement content can lead to SiC particles chaining together, creating a shorter path for the stress to travel, as evidenced by Figure 4.2.

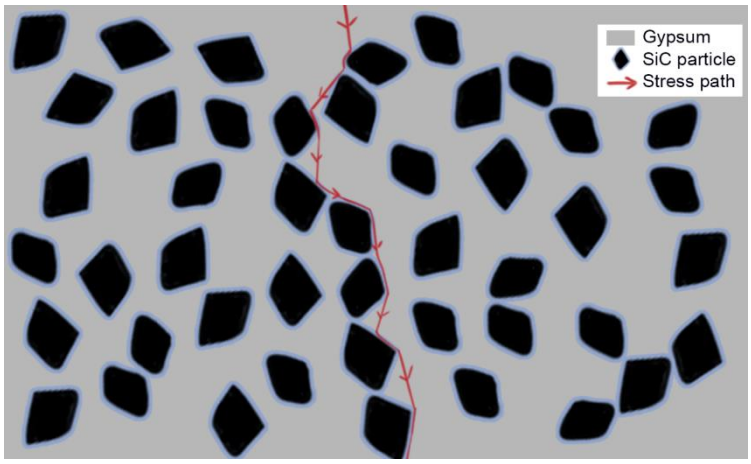

Figure 4.2 Effect of SiC particles and their interfaces past the reinforcement saturation point.

Imbuing gypsum with a strong reinforcement to further increase their performance and energy saving capabilities has proven beneficial. Other construction materials may also benefit from adding silicon carbide into the mixture to benefit its mechanical properties, especially if said material is either dark in colour by nature, the darkening and surface roughness increase isn't relevant, or an external layer can be applied with no significant impact in costs.

The gypsum-SiC composite's quality can be assessed with three-point flexural testing followed by microscopy on the fracture site to assess reinforcement distribution.

BIBLIOGRAPHY

[1] E. A. C., "INTRODUCTION TO COMPOSITES MATERIALS HULL." Accessed: Aug. 25, 2023. [Online]. Available: https://www.academia.edu/73858336/INTRODUCTION_TO_COMPOSITES_MATERIALS_HULL

[2] "Handbook of Ceramic Composites," *Handbook of Ceramic Composites*, 2005, doi: 10.1007/B104068.

[3] W. Krenkel, "Ceramic Matrix Composites: Fiber Reinforced Ceramics and their Applications," *Ceramic Matrix Composites: Fiber Reinforced Ceramics and their Applications*, pp. 1–418, Jun. 2008, doi: 10.1002/9783527622412.

[4] K. Cui *et al.*, "Microstructure, mechanical properties, and reinforcement mechanism of carbide toughened ZrC-based ultra-high temperature ceramics: A review," *https://doi.org/10.1080/09276440.2021.2012409*, vol. 29, no. 7, pp. 729–748, 2022, doi: 10.1080/09276440.2021.2012409.

[5] X. Zhang, L. Xu, W. Han, L. Weng, J. Han, and S. Du, "Microstructure and properties of silicon carbide whisker reinforced zirconium diboride ultra-high temperature ceramics," *Solid State Sci*, vol. 11, no. 1, pp. 156–161, Jan. 2009, doi: 10.1016/J.SOLIDSTATESCIENCES.2008.05.010.

[6] H. Mao *et al.*, "Microstructure and Mechanical Properties of Carbide Reinforced TiC-Based Ultra-High Temperature Ceramics: A Review," *Coatings 2021, Vol. 11, Page 1444*, vol. 11, no. 12, p. 1444, Nov. 2021, doi: 10.3390/COATINGS11121444.

[7] N. Kondratieva, M. Barre, F. Goutenoire, M. Sanytsky, and A. Rousseau, "Effect of additives SiC on the hydration and the crystallization processes of gypsum," *Constr Build Mater*, vol. 235, p. 117479, Feb. 2020, doi: 10.1016/J.CONBUILDMAT.2019.117479.

[8] J. Dweck and E. I. P. Lasota, "Quality control of commercial plasters by thermogravimetry," *Thermochim Acta*, vol. 318, no. 1–2, pp. 137–142, Sep. 1998, doi: 10.1016/S0040-6031(98)00338-4.

[9] "Standard Test Methods for Flexural Properties of Unreinforced and Reinforced Plastics and Electrical Insulating Materials 1."

[10] "Standard Test Method for Flexural Properties of Continuous Fiber-Reinforced Advanced Ceramic Composites 1."

[11] R. M. Gonçalves, "Avaliação da potencial utilização de fibras de vidro recicladas para o desenvolvimento de compósitos à base de gesso."

[12] "TGA-DSC analysis of silicon carbide: (a) TG-DTG curves, (b) TG-DSC curves | Download Scientific Diagram." Accessed: Sep. 17, 2023. [Online]. Available: https://www.researchgate.net/figure/TGA-DSC-analysis-of-silicon-carbide-a-TG-DTG-curves-b-TG-DSC-curves_fig3_283933073

[13] D. C. Engbrecht and D. A. Hirschfeld, "Thermal analysis of calcium sulfate dihydrate sources used to manufacture gypsum wallboard," *Thermochim Acta*, vol. 639, pp. 173–185, Sep. 2016, doi: 10.1016/J.TCA.2016.07.021.

[14] R. S. Duryat, "Evaluation of C/C-SiC Composites as Potential Candidate Materials for High Performance Braking Systems," *IOP Conf Ser Mater Sci Eng*, vol. 131, no. 1, Jun. 2016, doi: 10.1088/1757-899X/131/1/012009.

[15] N. Smaoui, M. A. Bérubé, B. Fournier, and B. Bissonnette, "Influence of Specimen Geometry, Orientation of Casting Plane, and Mode of Concrete Consolidation on Expansion Due to ASR," *Cement, Concrete, and Aggregates*, vol. 26, no. 2, p. CCA11927, Dec. 2004, doi: 10.1520/CCA11927.

[16] F. Iucolano, L. Boccarusso, and A. Langella, "Hemp as eco-friendly substitute of glass fibres for gypsum reinforcement: Impact and flexural behaviour," *Compos B Eng*, vol. 175, p. 107073, Oct. 2019, doi: 10.1016/J.COMPOSITESB.2019.107073.

[17] K. Daviau and K. K. M. Lee, "Decomposition of silicon carbide at high pressures and temperatures," *Phys Rev B*, vol. 96, p. 174102, 2017, doi: 10.1103/PhysRevB.96.174102.

[18] K. Ghazi Wakili, E. Hugi, L. Wullschleger, and T. Frank, "Gypsum board in fire - Modeling and experimental validation," *J Fire Sci*, vol. 25, no. 3, pp. 267–282, May 2007, doi: 10.1177/0734904107072883.

A

Appendix

A.1 Further Stress-Strain graphics

All results for three-point flexural tests can be seen below, starting with testing of sample performance over time. Percentages of SiC (V/V) and time periods are presented.

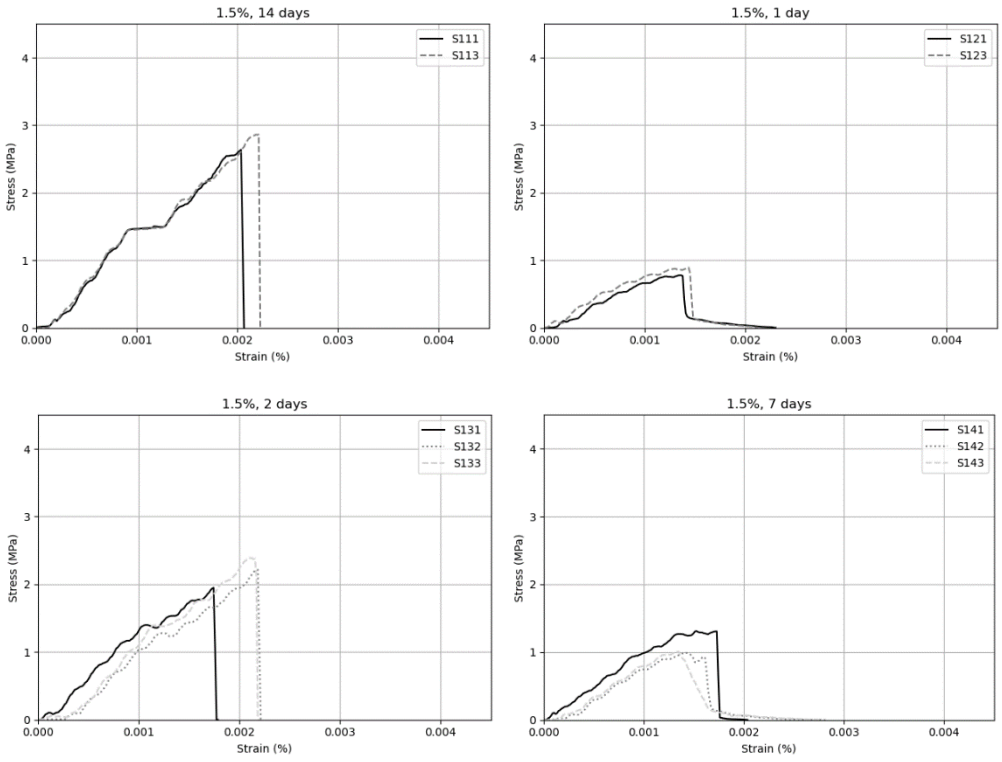

Figure 4.3 Performance over time testing 1,5 %(V/V) SiC - part 1.

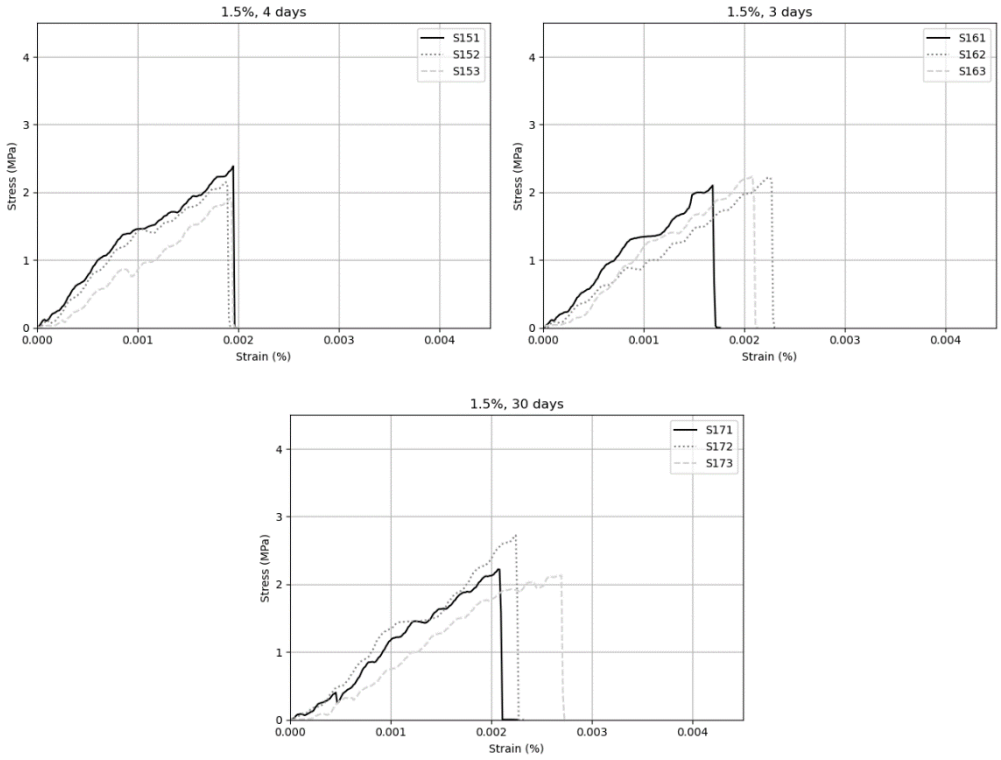

Figure 4.4 Performance over time testing 1,5 %(V/V) SiC - part 2.

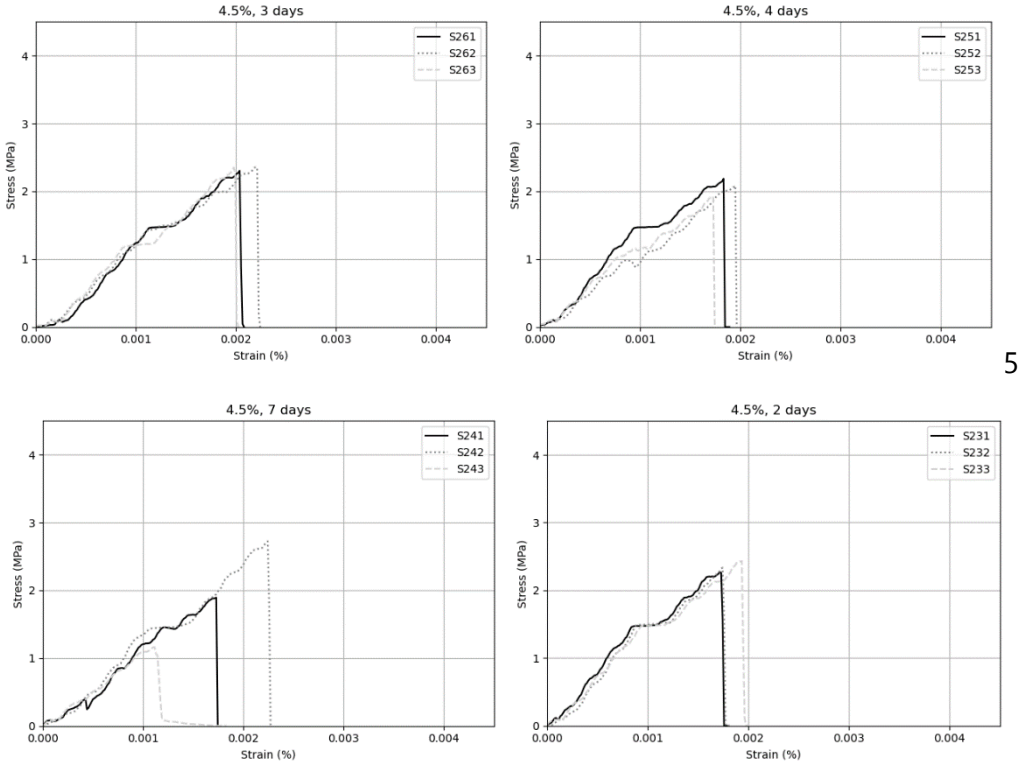

Figure 4.5 Performance over time testing 4,5 %(V/V) SiC - part 1.

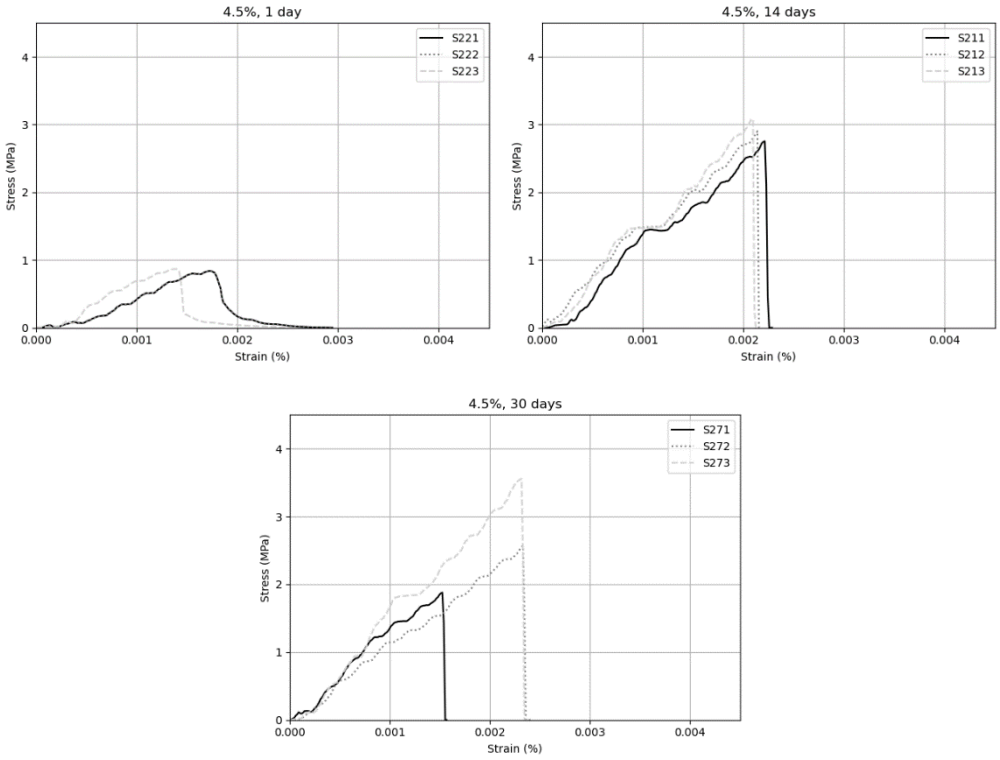

Figure 4.6 Performance over time testing 4,5 %(V/V) SiC - part 2.

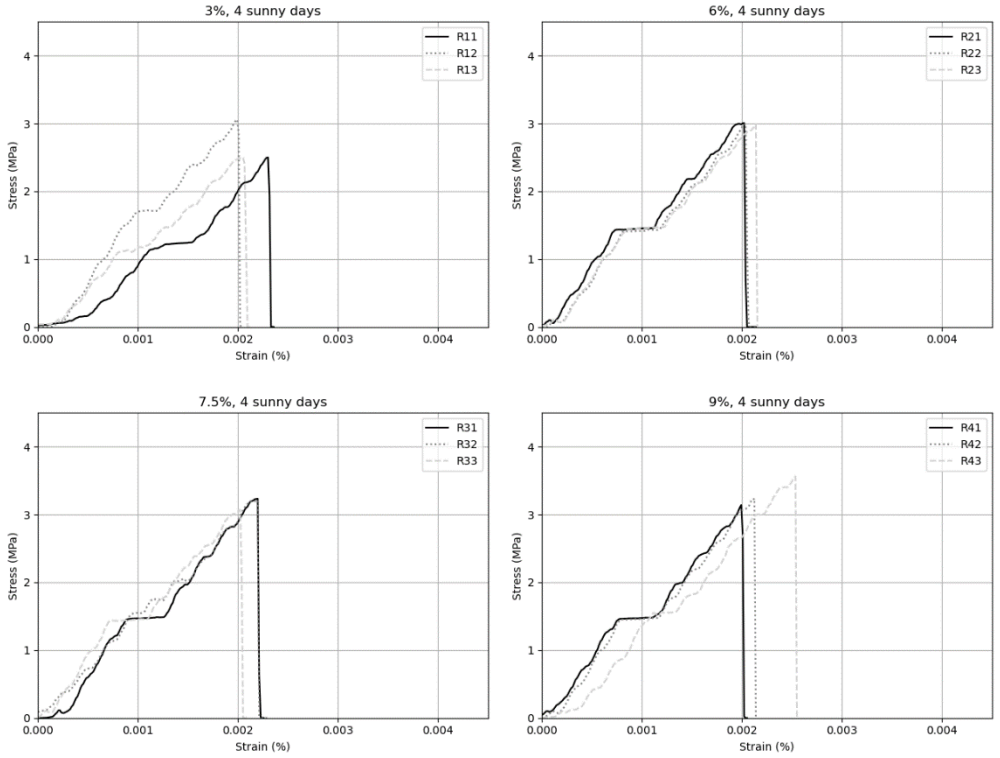

Figure 4.7 Performance over concentration testing - part 1.

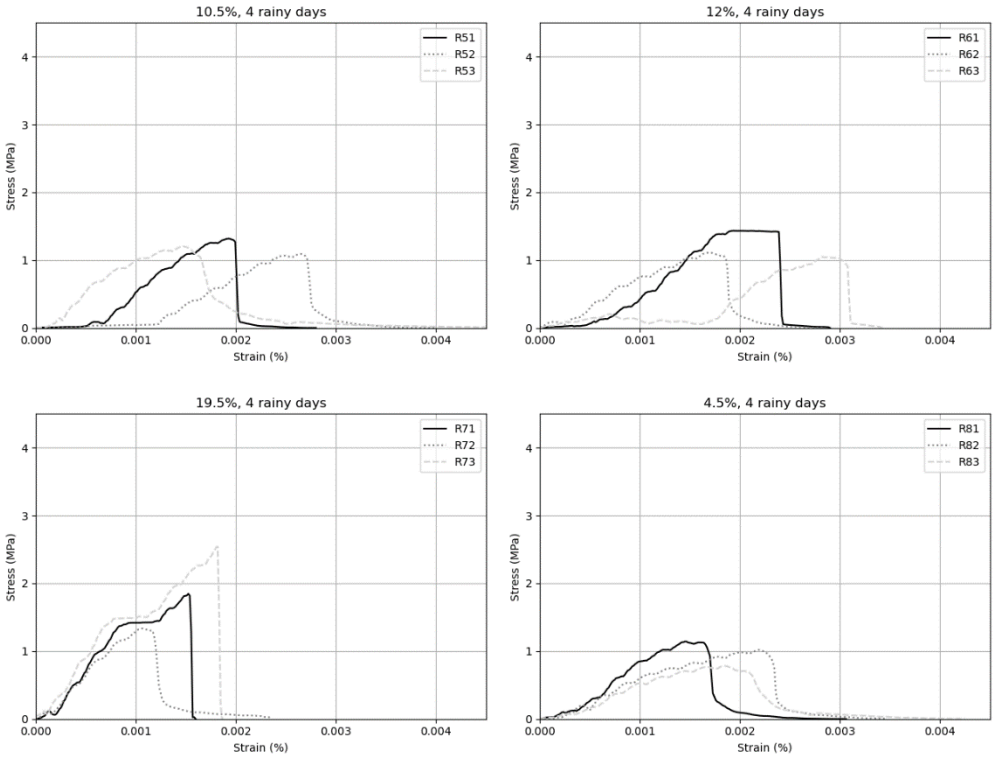

Figure 4.8 Performance over concentration testing - part 2.

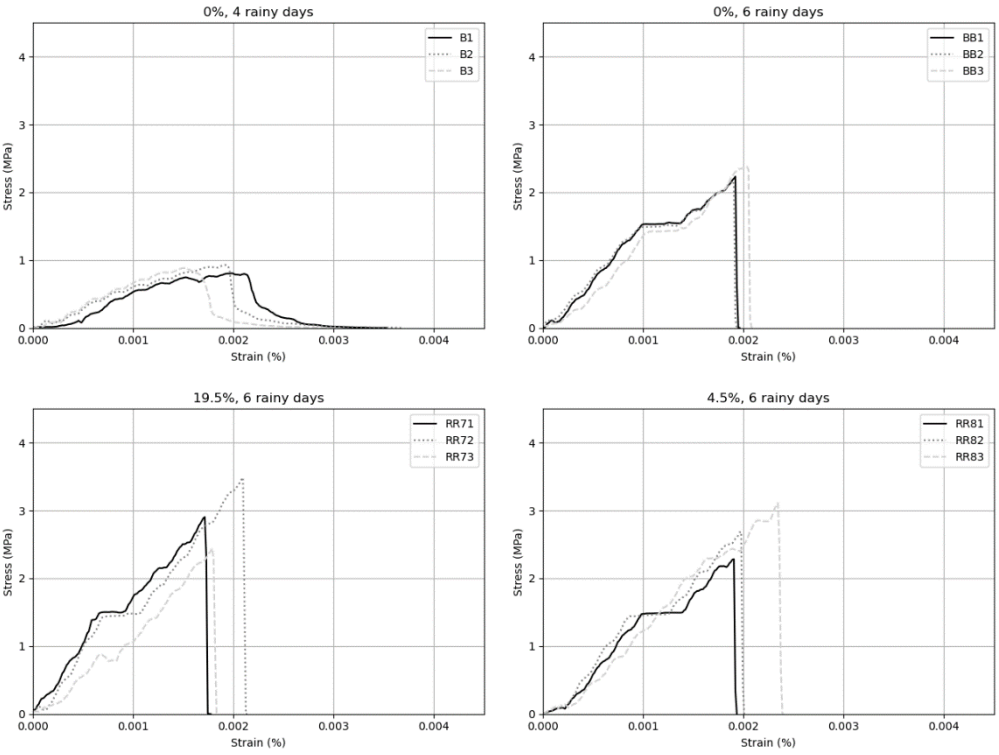

Figure 4.9 Performance over concentration testing - part 3.

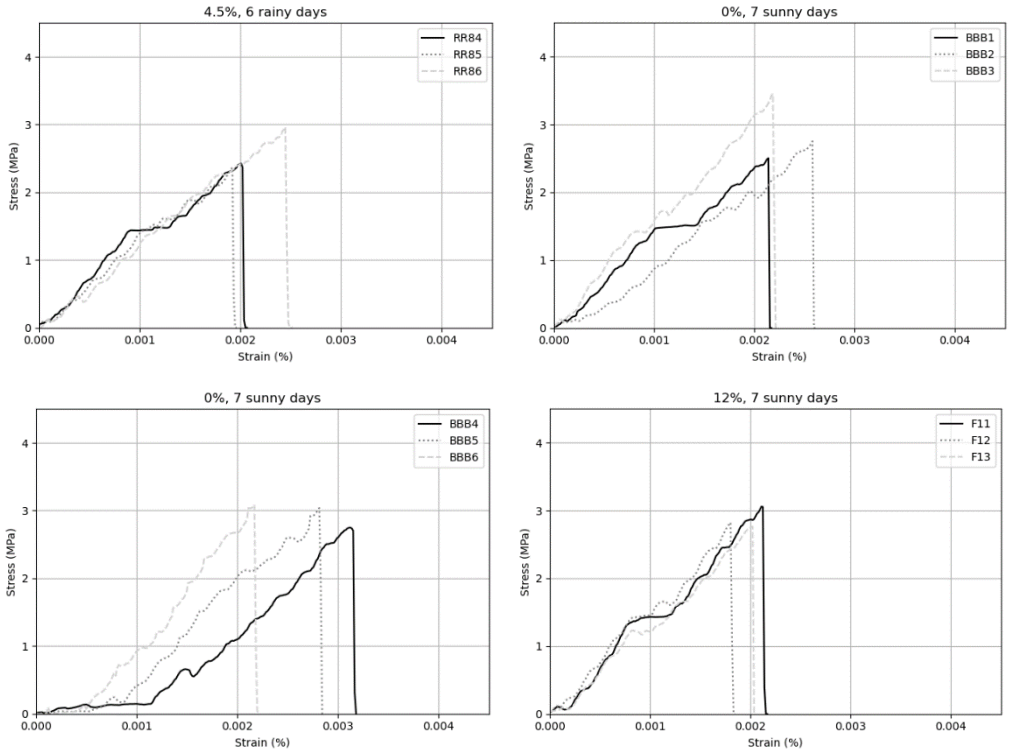

Figure 4.10 Performance over concentration testing - part 4.

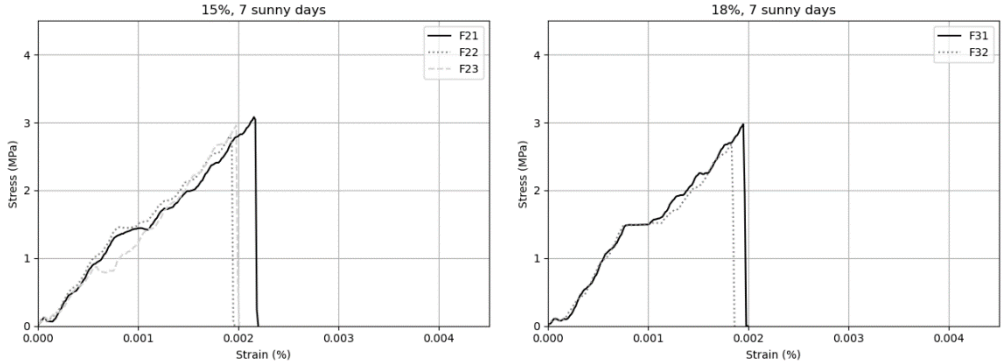

Figure 4.11 Performance over concentration testing - part 5.

A.2 Further Optical Microscopy Images

Additional optical microscopy images can be seen below.

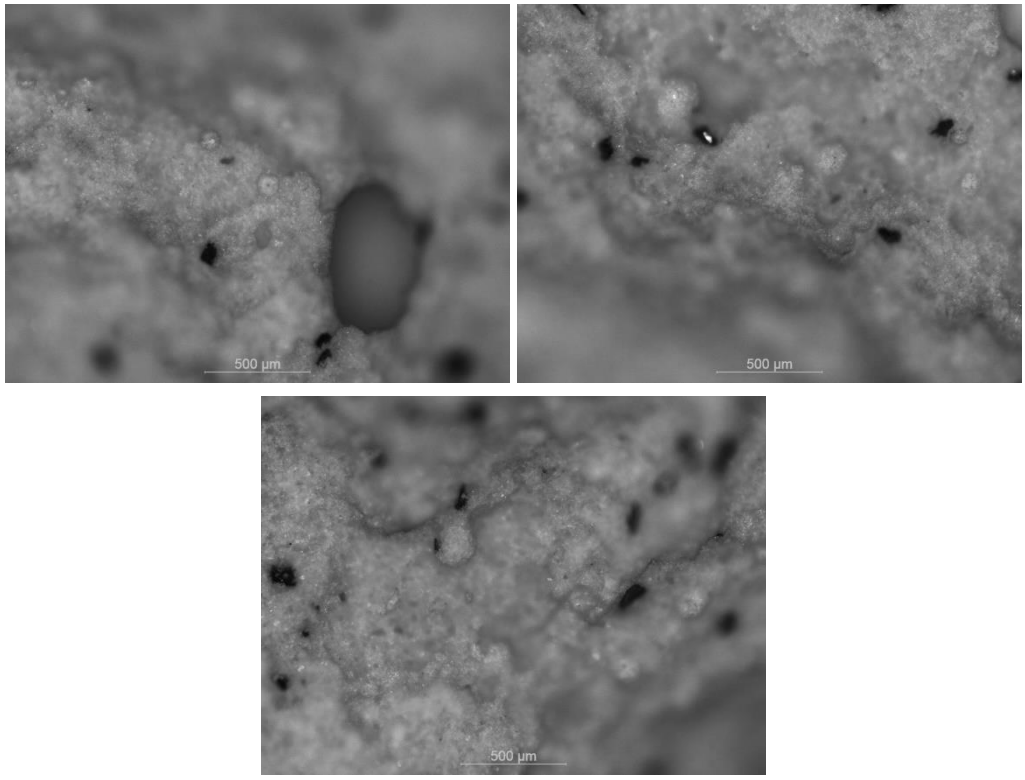

Figure 4.12 Additional low-performing 1,5 %(V/V) SiC sample optical microscopy pictures.

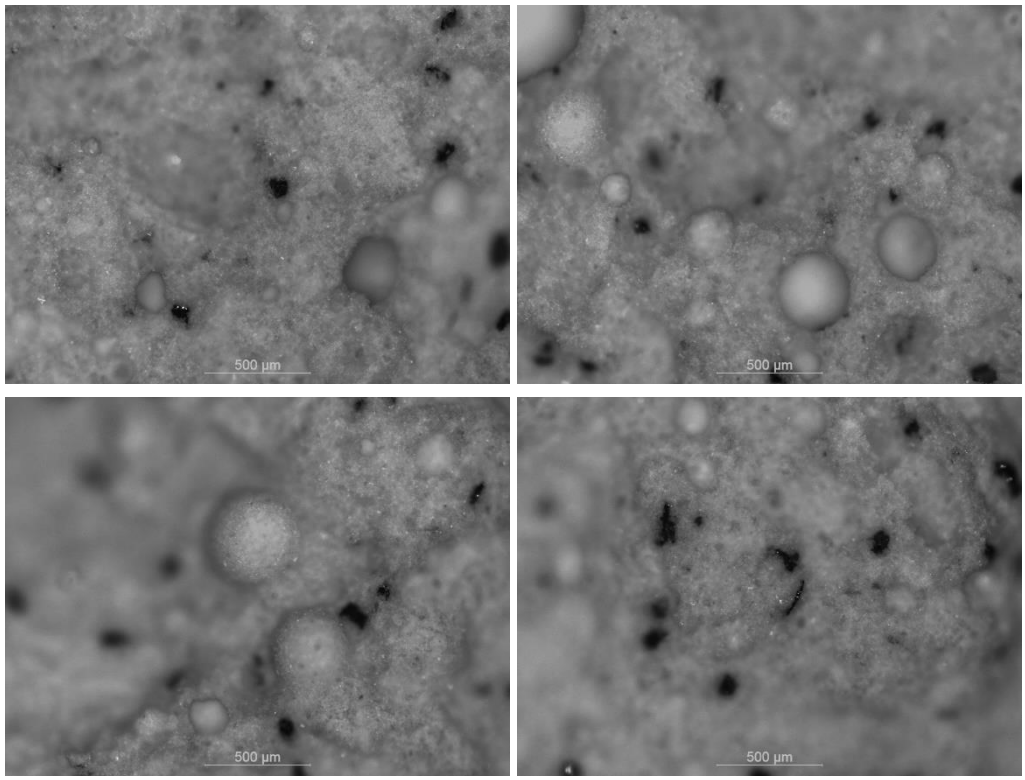

Figure 4.13 Additional high-performing 1,5 %(V/V) SiC sample optical microscopy pictures - part 1.

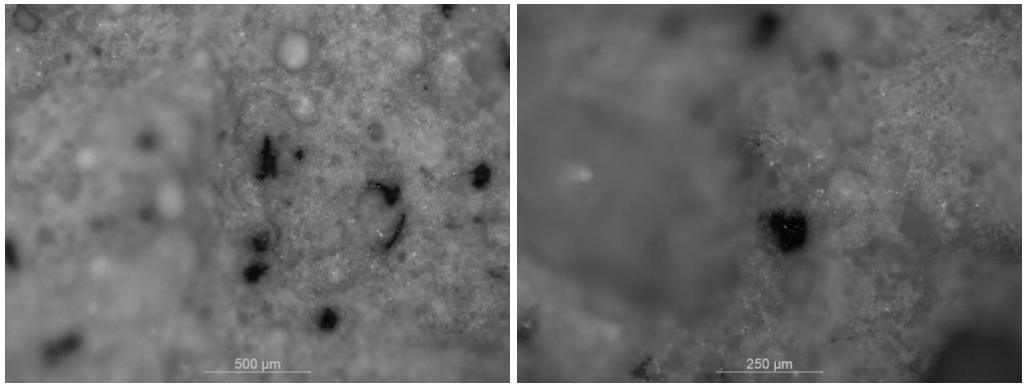

Figure 4.14 Additional high-performing 1,5 %(V/V) SiC sample optical microscopy pictures - part 2.

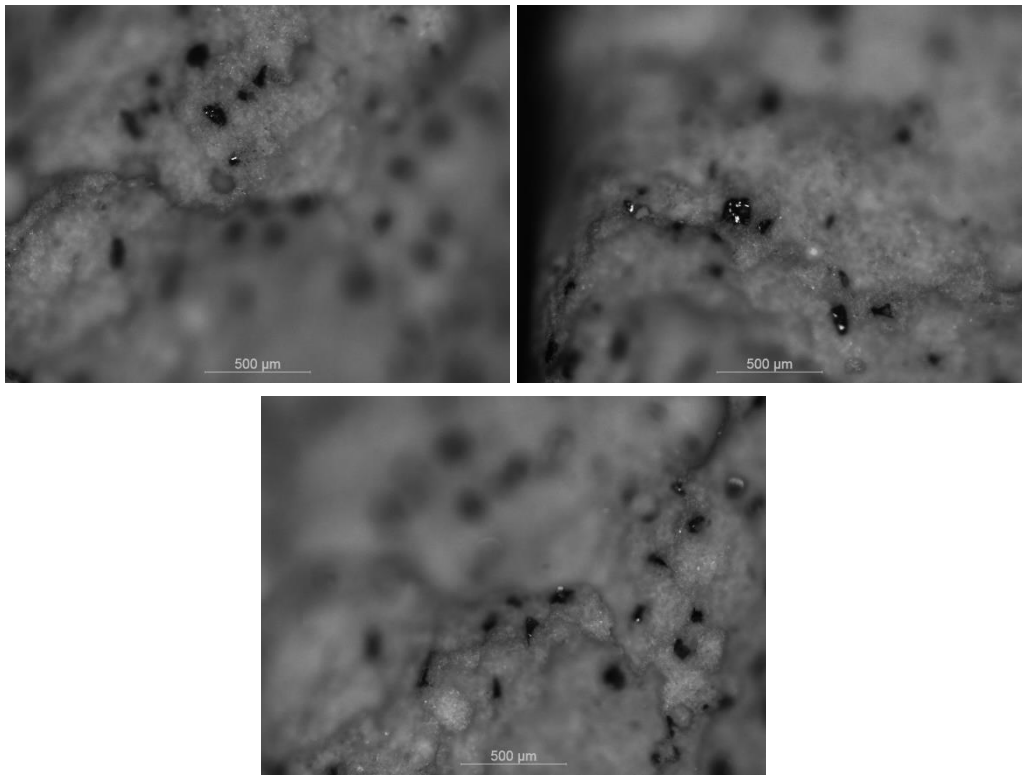

Figure 4.15 Additional low-performing 4,5 %(V/V) SiC sample optical microscopy pictures.

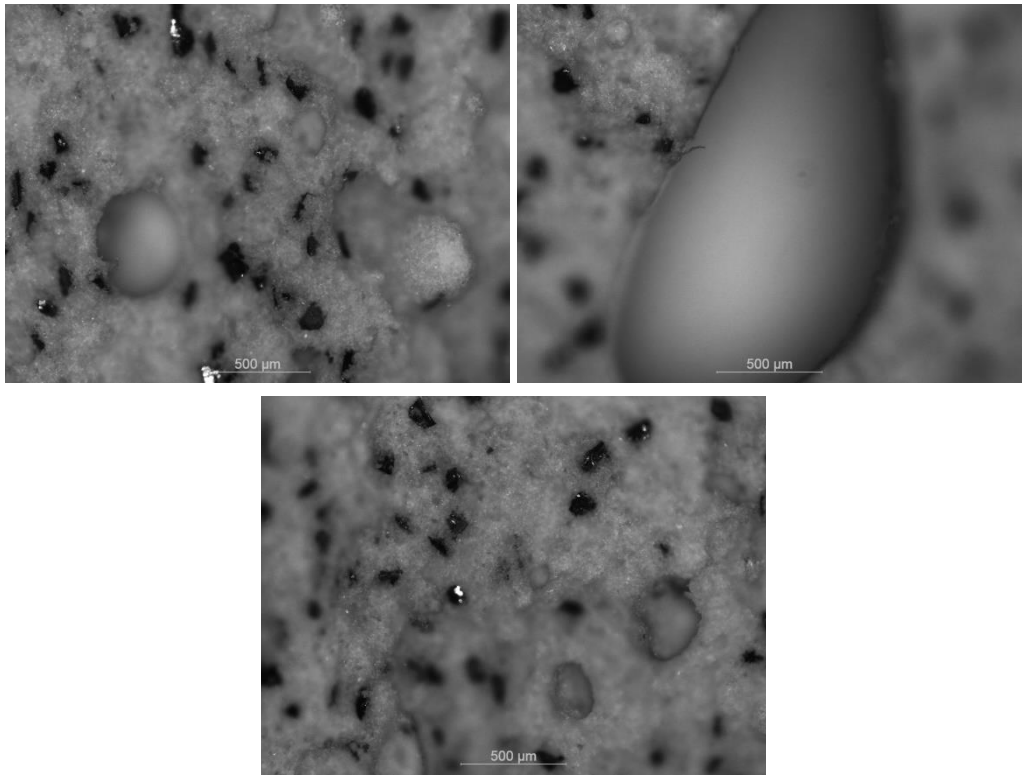

Figure 4.16 Additional high-performing 4,5 %(V/V) SiC sample optical microscopy pictures - part 1.

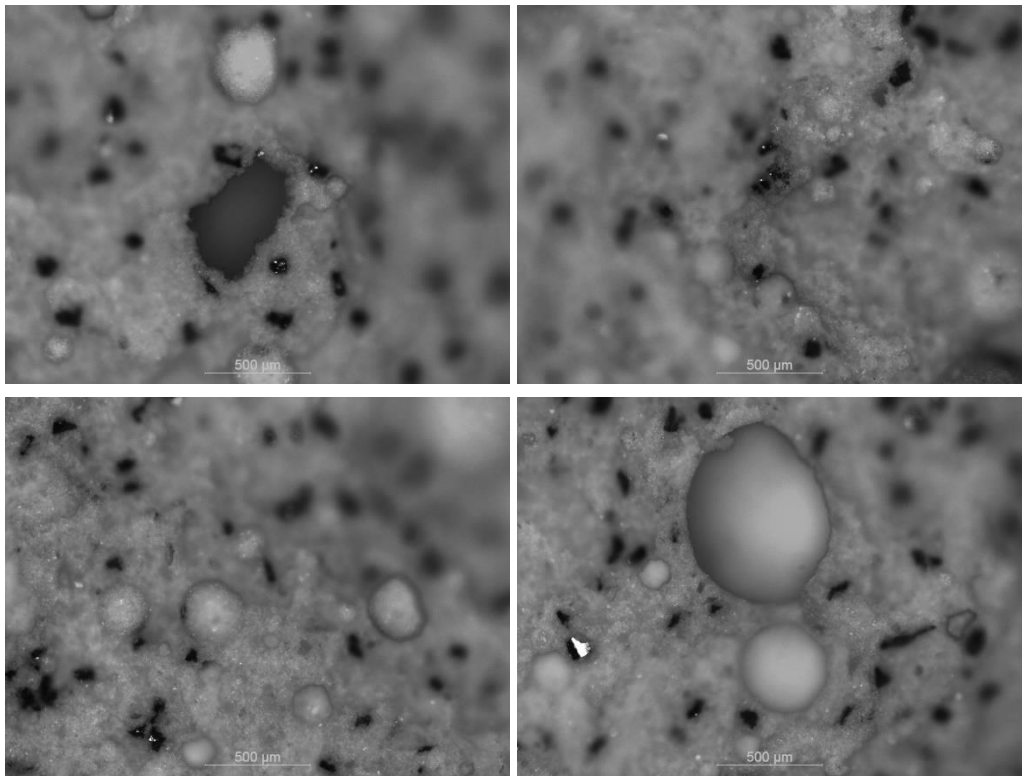

Figure 4.17 Additional high-performing 4,5 %(V/V) SiC sample optical microscopy pictures - part 2.

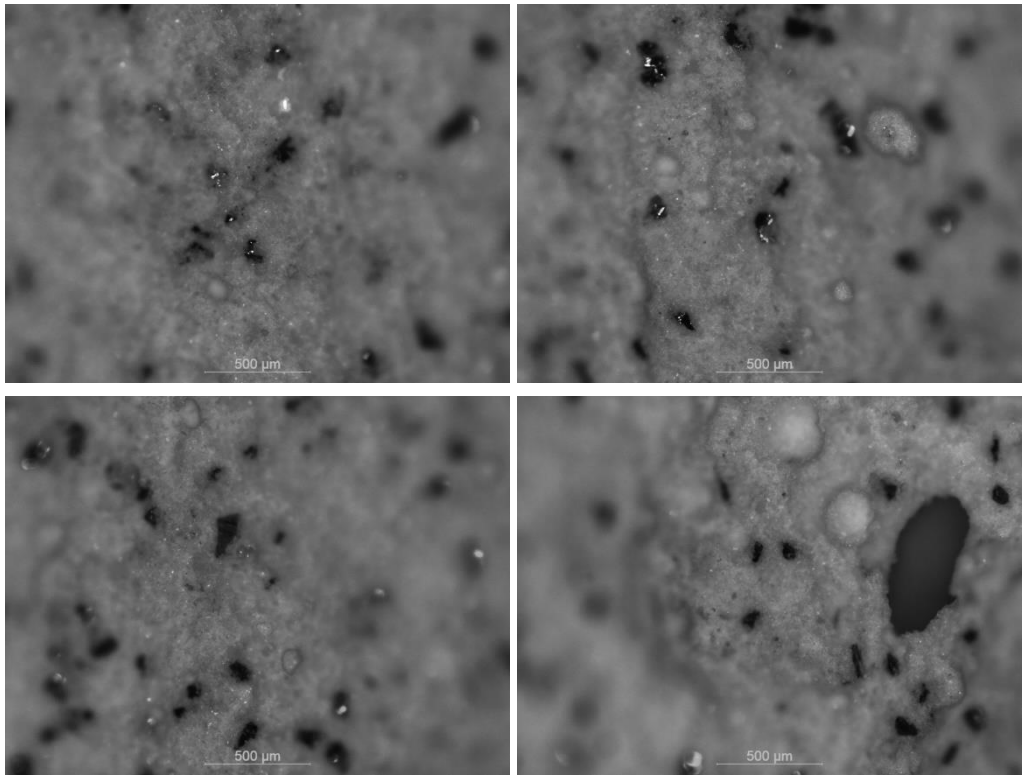

Figure 4.18 Additional high-performing 4,5 %(V/V) SiC sample optical microscopy pictures - part 3.

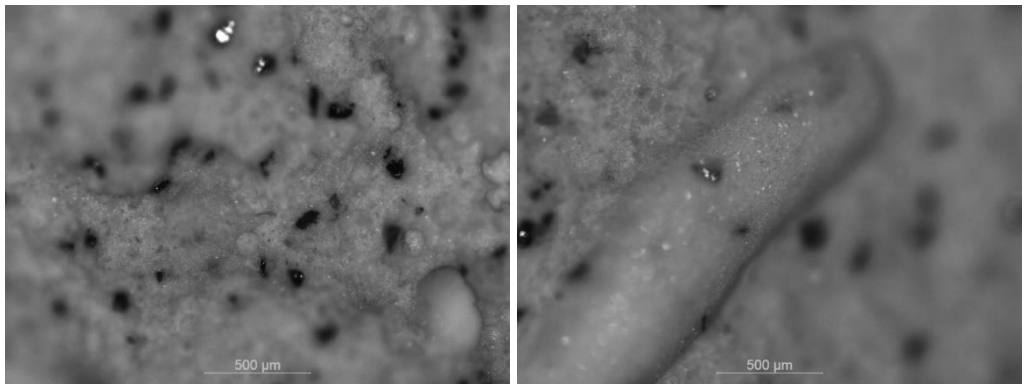

Figure 4.19 Additional high-performing 4,5 %(V/V) SiC sample optical microscopy pictures - part 4.

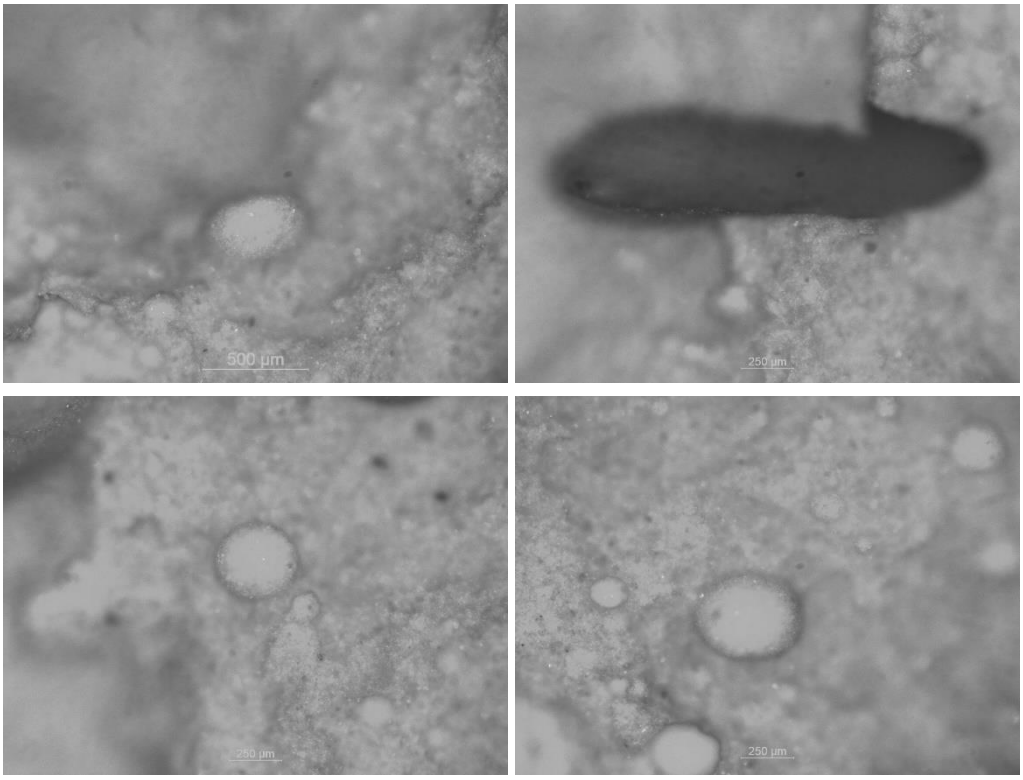

Figure 4.20 Additional pure gypsum optical microscopy pictures - part 1.

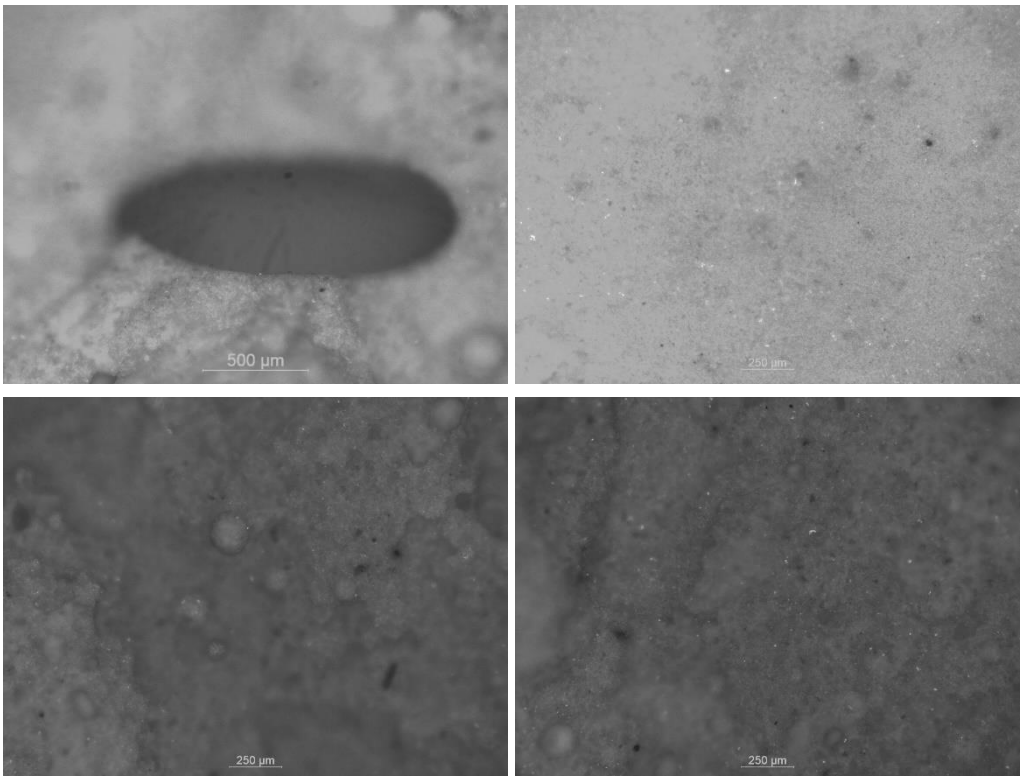

Figure 4.21 Additional pure gypsum optical microscopy pictures - part 2.

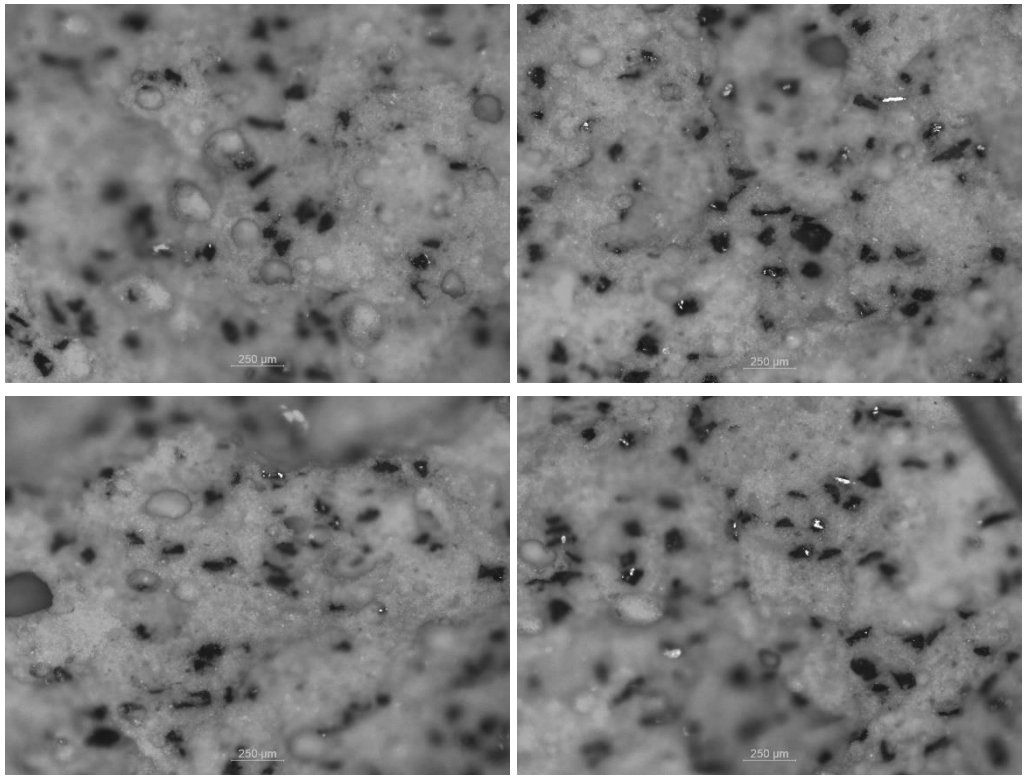

Figure 4.22 Additional 9 %(V/V) SiC sample optical microscopy pictures - part 1.

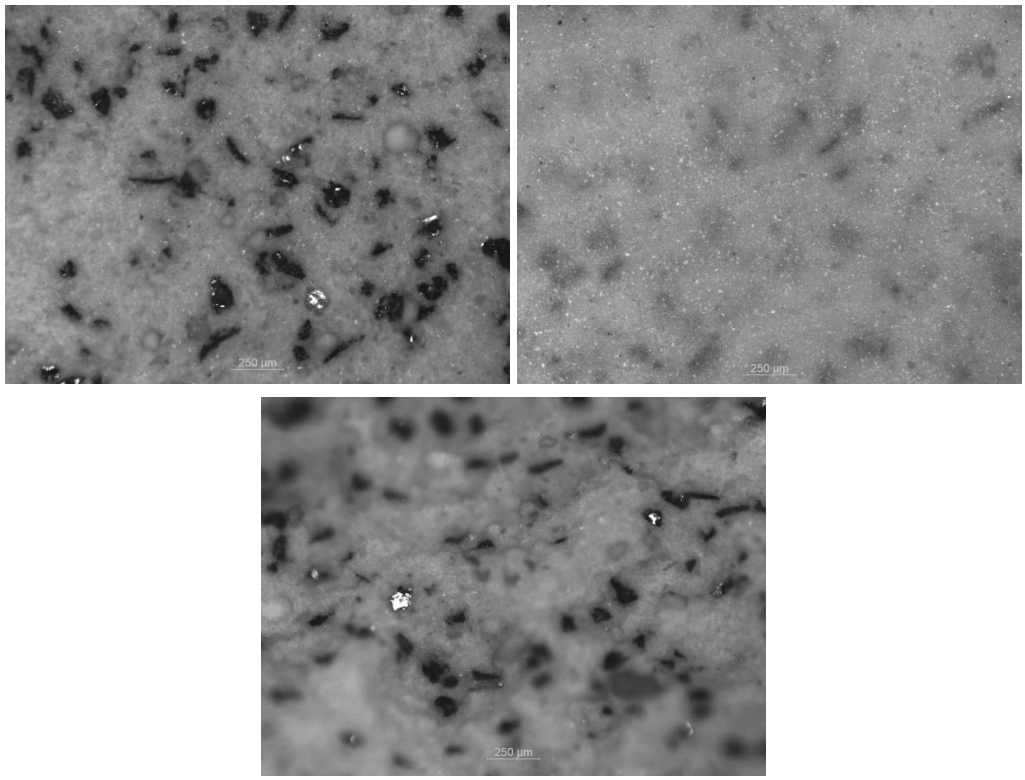

Figure 4.23 Additional 9 %(V/V) SiC sample optical microscopy pictures - part 2.

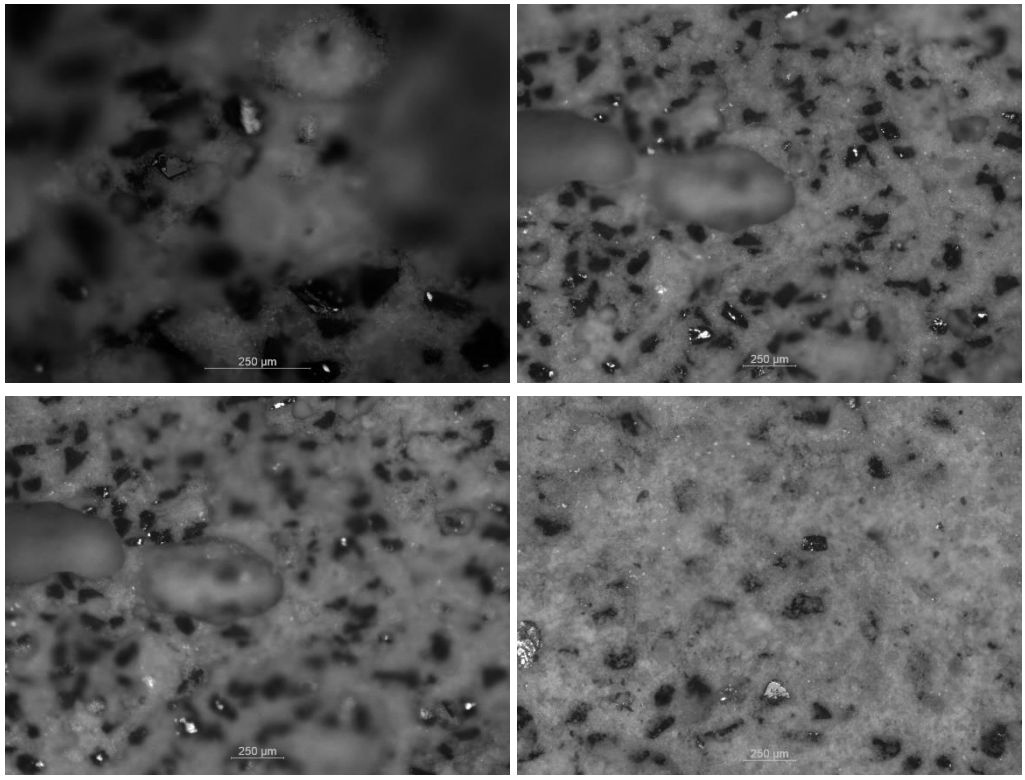

Figure 4.24 Additional low-performing 19,5 %(V/V) SiC sample optical microscopy pictures - part 1.

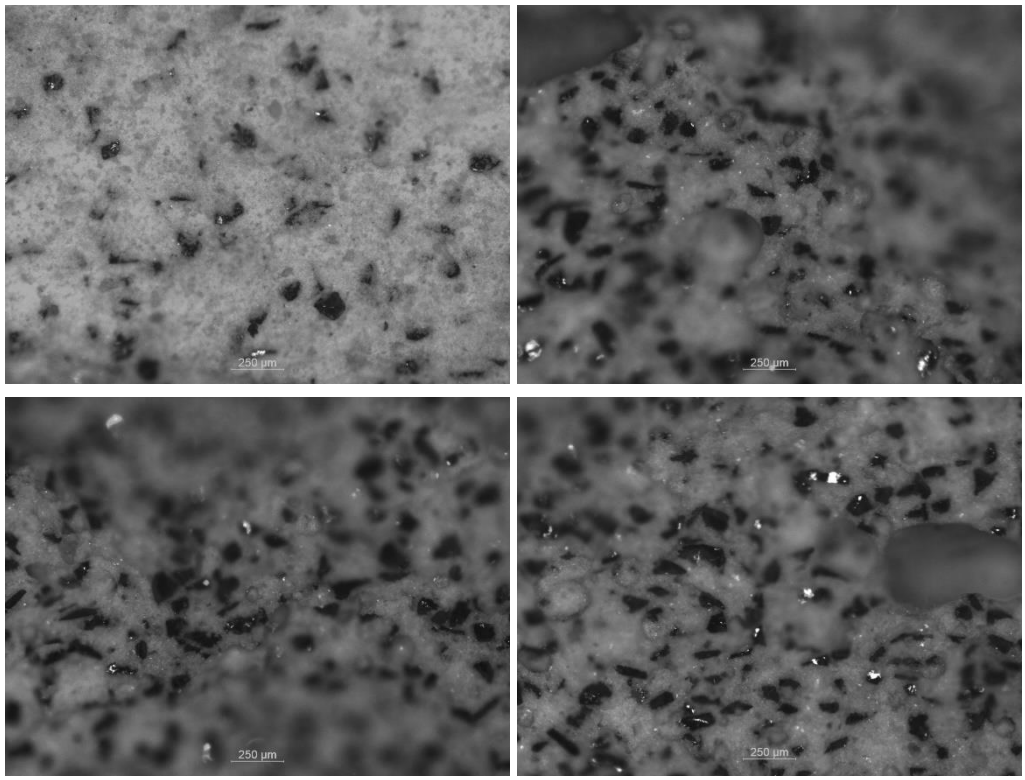

Figure 4.25 Additional low-performing 19,5 %(V/V) SiC sample optical microscopy pictures - part 2.

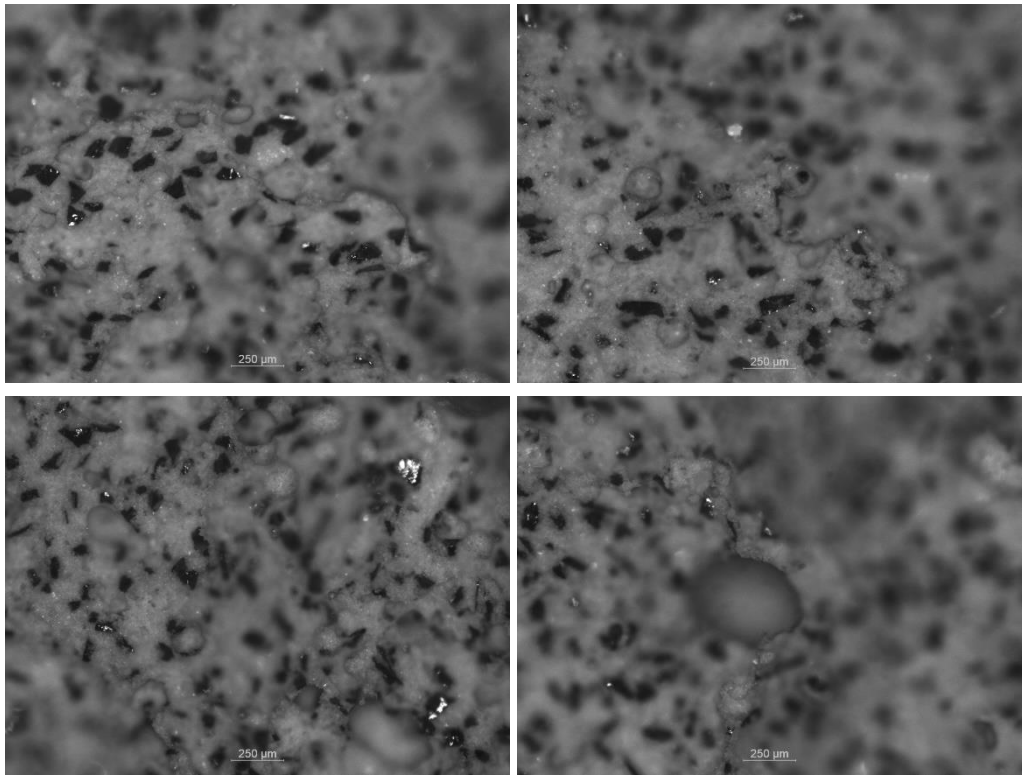

Figure 4.26 Additional high-performing 19,5 %(V/V) SiC sample optical microscopy pictures - part 1.

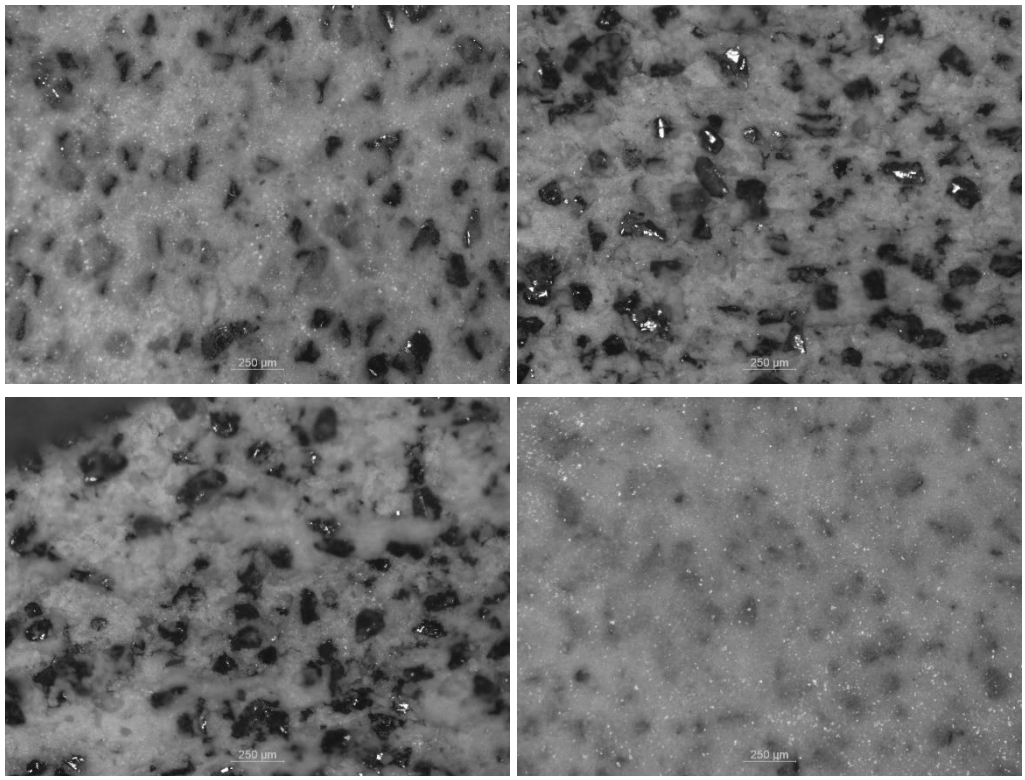

Figure 4.27 Additional high-performing 19,5 %(V/V) SiC sample optical microscopy pictures - part 2.

A.3 Further SEM Images

Additional SEM images can be seen below.

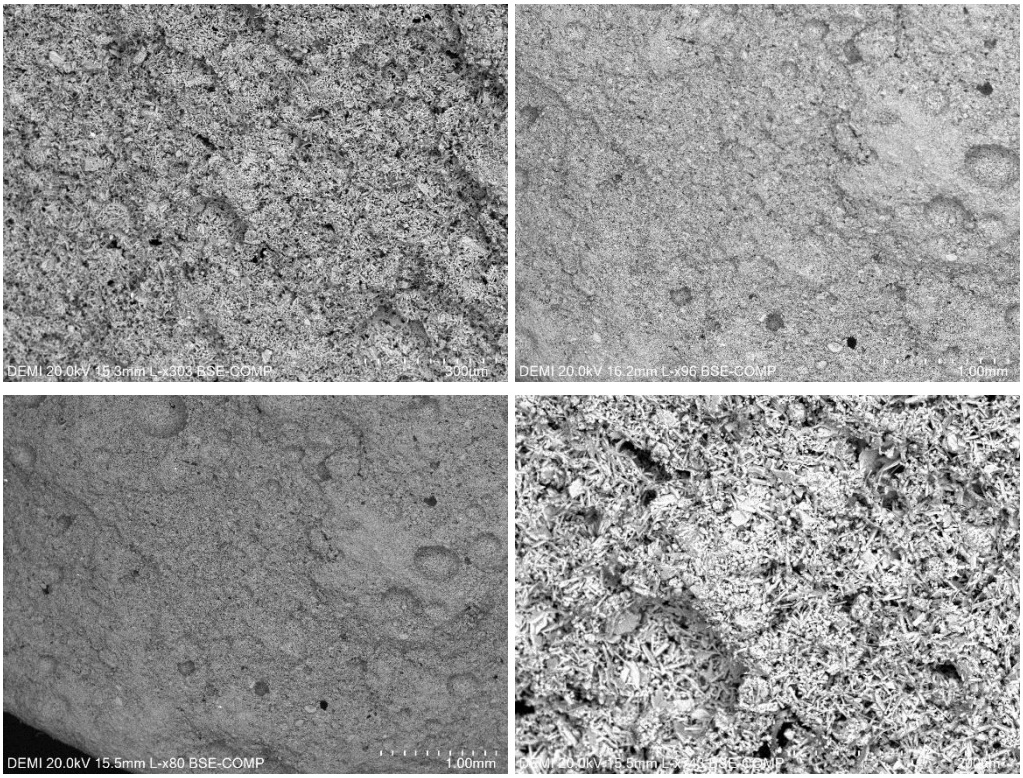

Figure 4.28 Additional pure gypsum SEM images.

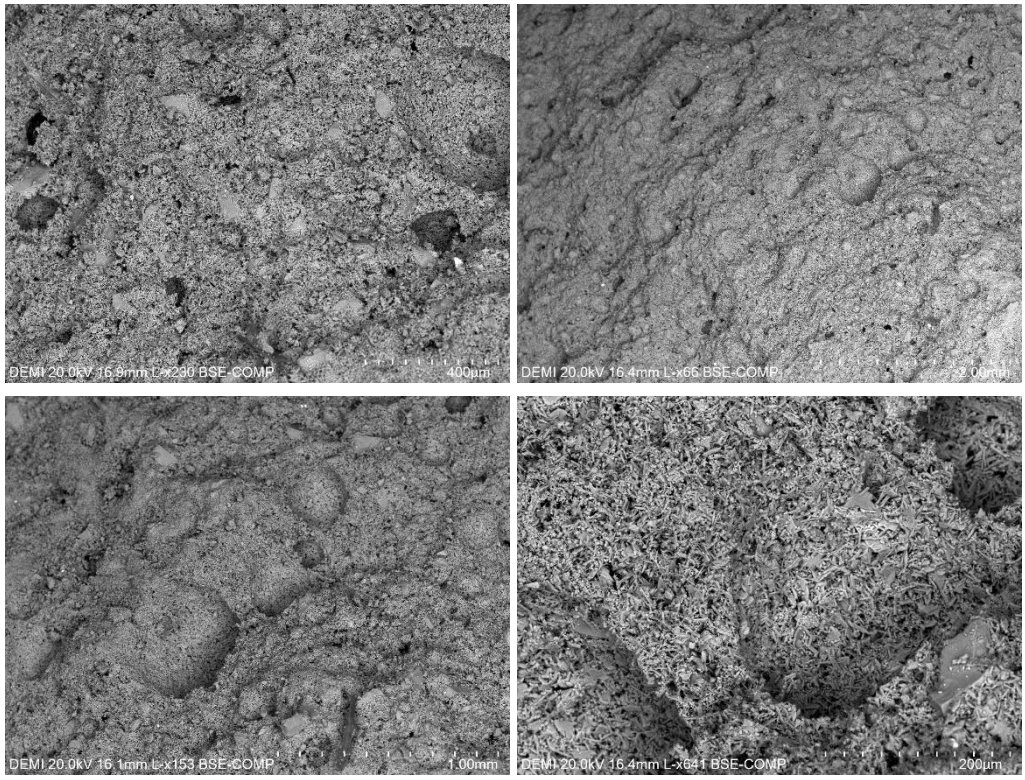

Figure 4.29 Additional 9 %(V/V) SiC sample SEM images.

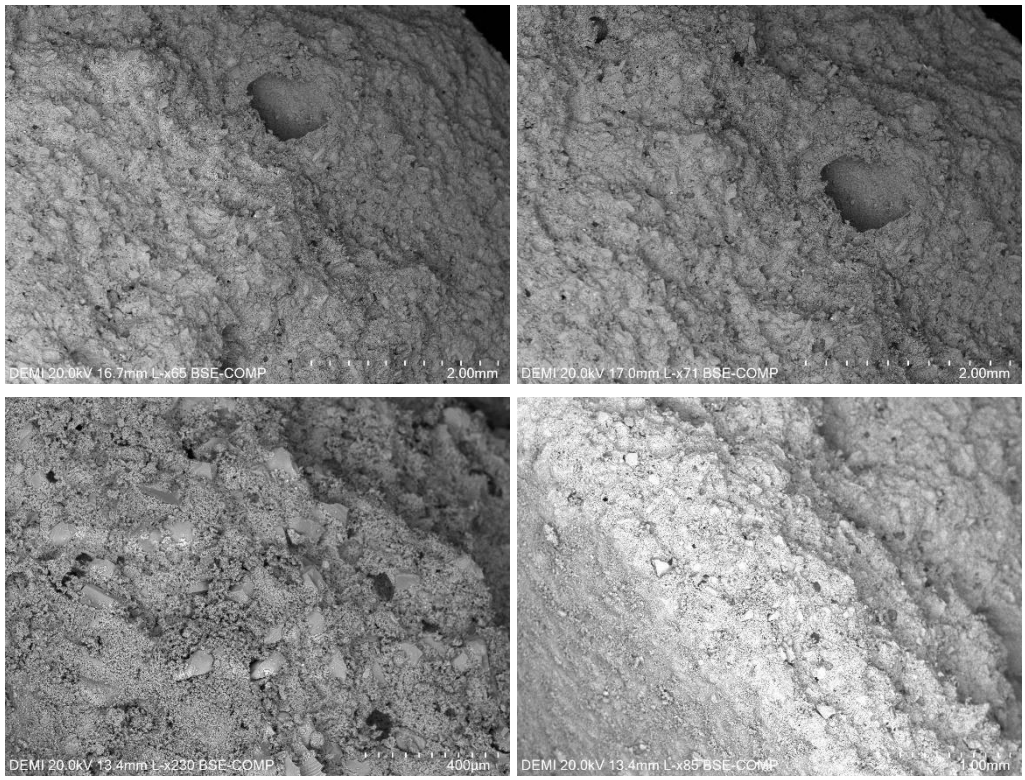

Figure 4.30 Additional 19,5 %(V/V) SiC sample SEM images - part 1.

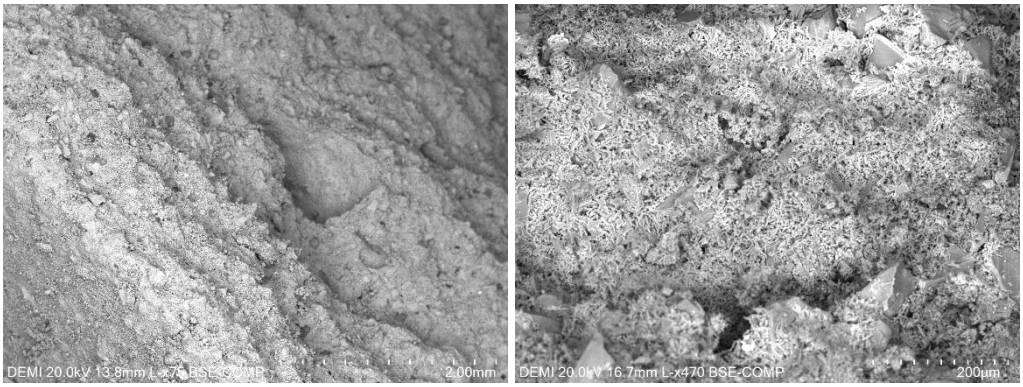

Figure 4.31 Additional 19,5 %(V/V) SiC sample SEM images - part 2.

2023

DENIS COMLEV

MICROSTRUCTURE AND MECHANICAL PROPERTIES OF CERAMICS REINFORCED WITH RECYCLED WASTE